

Storage Stability and Phase Separation Behaviour of Polymer-Modified Bitumen

Characterization and Modelling

Jiqing Zhu

Doctoral Thesis
KTH Royal Institute of Technology
School of Architecture and the Built Environment
Department of Civil and Architectural Engineering
SE-100 44 Stockholm, Sweden

TRITA-BKN. BULLETIN 143, 2016
ISSN 1103-4270
ISRN KTH/BKN/B-143-SE
ISBN 978-91-7729-187-9

© Jiqing Zhu
Stockholm 2016

Akademisk avhandling som med tillstånd av KTH i Stockholm framlägges till offentlig
granskning för avläggande av teknologie doktorsexamen tisdagen den 22 november kl.
10:00 i Kollegiesalen, KTH, Brinellvägen 8, Stockholm.

Abstract

Polymer-modified bitumen (PMB) is a high-performance material for road construction and maintenance. But its storage stability and phase separation behaviour are still not sufficiently understood and need to be studied toward a more successful and sustainable application of PMB. In this thesis, the equilibrium thermodynamics and phase separation dynamics of PMB are investigated with the aim at a fundamental understanding on PMB storage stability and phase separation behaviour. The development of polymer modifiers for paving bitumen is reviewed. The phase separation process in unstable PMBs is captured by fluorescence microscopy at the storage temperature (180 °C). A coupled phase-field model of diffusion and flow is developed to simulate and predict the PMB storage stability and phase separation behaviour. The temperature dependency of PMB phase separation behaviour is modelled by introducing temperature-dependent model parameters between 140 °C and 180 °C. This model is implemented in a finite element software package and calibrated with the experimental observations of real PMBs. The results indicate that storage stability and phase separation behaviour of PMB are strongly dependent on the specific combination of the base bitumen and polymer. An unstable PMB starts to separate into two phases by diffusion, because of the poor polymer-bitumen compatibility. Once the density difference between the two phases becomes sufficiently significant, gravity starts to drive the flow of the two phases and accelerates the separation in the vertical direction. The proposed model, based on the Cahn-Hilliard equation, Flory-Huggins theory and Navier-Stokes equations, is capable of capturing the stability differences among the investigated PMBs and their distinct microstructures at different temperatures. The various material parameters of the PMBs determine the differences in the phase separation behaviour in terms of stability and temperature dependency. The developed model is able to simulate and explain the resulting differences due to the material parameters. The outcome of this study may thus assist in future efforts of ensuring storage stability and sustainable application of PMB.

Keywords

Polymer-modified bitumen; Storage stability; Phase separation;
Fluorescence microscopy; Phase-field modelling

Sammanfattning

Polymermodifierade bitumen (PMB) är ett högpresterande material för väganläggning och underhåll. Men PMB:s lagringsstabilitet och fassepareringsegenskaper är inte tillräckligt förstådda än och behöver studeras för en mer framgångsrik och hållbar användning av PMB. I denna avhandling studeras termodynamisk jämvikt och fasseparation av PMB med målsättning att uppnå en grundläggande förståelse av PMB:s lagringsstabilitet och fassepareringsegenskaper. Utvecklingen av polymermodifierade bitumen sammanfattas. Fasseparationsprocessen av instabil PMB:s studeras med hjälp av fluorescens mikroskop vid lagringstemperatur (180°C). En kopplad fas-fälts modell som beskriver diffusion och flöde har utvecklats för att simulera och förutsäga PMB:s lagringsstabilitet och fassepareringsegenskaper. Temperaturberoendet hos PMB:s fasseparation har beskrivits genom att införa temperaturberoende modellparametrar mellan 140°C och 180°C . Denna modell är införd i ett finit element program och kalibrerad med experimentella observationer på verkliga PMB. Resultaten indikerar att lagringsstabiliteten och fasseparationen hos PMB är starkt beroende av den specifika kombinationen av basbitumen och polymer. En instabil PMB börjar separera i två faser genom diffusion, beroende på dålig bitumen-polymer kompatibilitet. När skillnaden i densitet mellan de två faserna blir tillräckligt stor kommer gravitationen att driva flödet av de två faserna och accelerera separationen i vertikalled. Den föreslagna modellen, baserad på Cahn-Hilliards ekvation, Flory-Huggins teori och Navier-Stokes ekvation, kan beskriva stabilitetsskillnaderna mellan de undersökta PMB:erna och deras distinkta mikrostruktur vid olika temperaturer. De olika materialparametrarna hos PMB bestämmer skillnaden i fassepareringsegenskaper i termer av stabilitet och temperaturberoende. Den utvecklade modellen kan simulera och förklara de resulterande skillnaderna på grund av materialparametrarna. Resultatet av denna studie kan bidra till att säkerställa lagringsstabilitet och hållbara applikationer för PMB.

Nyckelord

Polymermodifierad bitumen; Lagringsstabilitet; Fasseparation;
Fluorescensmikroskop; Fas-fälts modellering

Preface

The study presented in this thesis was carried out in the Highway Engineering Research Group in the Department of Civil and Architectural Engineering, KTH Royal Institute of Technology. I started this project with a scholarship from the China Scholarship Council. This study was also partially supported by the Nordiskt Vägforum, Trafikverket's BVFF program and the KTH Road2Science Center. All support is gratefully acknowledged.

First of all, I would like to thank my supervisor Associate Professor Nicole (Niki) Kringos for her guidance, support and encouragement during my study. I also wish to express my gratitude to Dr. Romain Balieu from KTH and Dr. Xiaohu Lu from Nynas AB for their expert advice and detailed comments on the work. Mr. Petri Uhlbäck and Mr. Bengt Sandman from Nynas AB are acknowledged for their assistance with the experiments. My appreciation is also extended to all my colleges at KTH and friends.

Last but not least, my special thanks go to my wife, my daughter and my family in China, for their support and love.

Jiqing Zhu

朱继青

Stockholm, September 2016

List of Publications

Appended Publications

This thesis is based on the following six journal papers:

Paper I

Zhu, J., Birgisson, B., & Kringos, N. (2014). Polymer modification of bitumen: Advances and challenges. *European Polymer Journal*, 54, 18-38.

Paper II

Zhu, J., & Kringos, N. (2015). Towards the development of a viscoelastic model for phase separation in polymer-modified bitumen. *Road Materials and Pavement Design*, 16(S1), 39-49.

Paper III

Zhu, J., Lu, X., & Kringos, N. (2016). Experimental investigation on storage stability and phase separation behaviour of polymer-modified bitumen. *International Journal of Pavement Engineering*, DOI:10.1080/10298436.2016.1211870.

Paper IV

Zhu, J., Lu, X., Balieu, R., & Kringos, N. (2016). Modelling and numerical simulation of phase separation in polymer modified bitumen by phase-field method. *Materials & Design*, 107, 322-332.

Paper V

Zhu, J., Balieu, R., Lu, X., & Kringos, N. (2016). Numerical investigation on phase separation in polymer modified bitumen: Effect of thermal condition. Submitted manuscript.

Paper VI

Zhu, J., Balieu, R., Lu, X., & Kringos, N. (2016). Numerically predicting storage stability of polymer-modified bitumen: A coupled model of gravity-driven flow and diffusion. Submitted manuscript.

(Authorship Statement: Jiqing Zhu is the first, corresponding and the only student author for all the above listed publications. He performed the literature review, designed the experiments, proposed the model, ran the simulations, analysed the results, drafted and revised all the papers.)

Additional Publications

Book chapter

Varveri, A., Zhu, J., & Kringos, N. (2015). Moisture damage in asphaltic mixtures. In S.-C. Huang, & H. Di Benedetto (Eds.), *Advances in Asphalt Materials: Road and Pavement Construction* (pp. 303-344). Cambridge, UK: Woodhead Publishing.

Licentiate thesis

Zhu, J. (2015). *Towards a Viscoelastic Model for Phase Separation in Polymer Modified Bitumen* (Licentiate thesis). KTH Royal Institute of Technology, Stockholm, Sweden.

Conference paper I

Zhu, J., Balieu, R., Lu, X., & Kringos, N. (2016). Characterization and modelling of phase separation in polymer modified bitumen. In R. Kádár (Ed.), *Annual Transactions of the Nordic Rheology Society: Papers Presented at the Nordic Rheology Conference*, Helsinki, Finland, 30 May - 1 June (vol. 24, pp. 59-61). Copenhagen, Denmark: Nordic Rheology Society.

Conference paper II

Zhu, J., Balieu, R., Lu, X., & Kringos, N. (2016). Influence of thermal history on phase separation in polymer modified bitumen: A numerical approach. In T. Pauli, & J.-P. Planche (Eds.), *Proceedings of the ISAP 2016 Symposium*, Jackson, Wyoming, USA, 18-21 July (paper 8). Lino Lakes, MN: International Society for Asphalt Pavements.

List of Abbreviations

EBA	Ethylene-butyl acrylate
EVA	Ethylene-vinyl acetate
LDPE	Low-density polyethylene
PB	Polybutadiene
PE	Polyethylene
PMB	Polymer-modified bitumen
PP	Polypropylene
PS	Polystyrene
R&B	Ring & Ball
SBS	Styrene-butadiene-styrene
SEBS	Styrene-ethylene/butylene-styrene
SHRP	Strategic Highway Research Program
SIS	Styrene-isoprene-styrene
TLC-FID	Thin-layer chromatography with flame ionization detection

Contents

Abstract	I
Sammanfattning	II
Preface	III
List of Publications	IV
List of Abbreviations.....	VI
1. Introduction.....	1
1.1. Background	1
1.2. Aims and Scope	2
1.3. Thesis Outline.....	3
2. State of the Art	4
2.1. Popular Polymers for Bitumen Modification.....	4
2.1.1. <i>Plastomers</i>	4
2.1.2. <i>Thermoplastic Elastomers</i>	8
2.2. PMB Storage Stability and Phase Separation.....	11
3. Experimental Characterization of PMB Storage Stability and Phase Separation	14
3.1. Materials and Method	14
3.2. Experimental Results and Analysis	16
3.3. Thermodynamics of PMB Phase Separation	19
4. Phase-Field Modelling of PMB Phase Separation at Storage Temperature	23
4.1. Phase-Field Model for PMB Phase Separation.....	23
4.2. Model Implementation and Parametric Studies.....	28
5. Temperature Dependency of PMB Phase Separation Behaviour: Numerical Study	36
5.1. Temperature Dependency of Model Parameters.....	36

5.2. Model Calibration for Real PMBs	37
5.3. Effect of Thermal Condition.....	41
<i>5.3.1. Effect of Temperature Level.</i>	41
<i>5.3.2. Effect of Cooling Rate.....</i>	46
6. Diffusion-Flow Coupling and Its Effect on PMB Storage Stability	51
6.1. Coupled Model of Diffusion and Flow.....	51
6.2. Model Parameters and Implementation	53
6.3. Numerical Simulation Results and Discussion	54
<i>6.3.1. PMB Storage Stability.....</i>	54
<i>6.3.2. Effect of Bitumen Density</i>	57
<i>6.3.3. Effect of Bitumen Dynamic Viscosity.....</i>	58
7. Conclusions and Recommendations.....	59
7.1. Conclusions.....	59
7.2. Recommendations	60
References	62
Appended Papers	71

1. Introduction

1.1. Background

Bitumen has been used for thousands of years as an engineering material. After the early 1900s, the world consumption of bitumen increased rapidly. Most of the consumed bitumen was used as the binder for road construction and maintenance (Asphalt Institute and Eurobitume, 2011). However, the crude oil resources for producing high-quality bitumen are limited and the demand on good road performance has increased during the last few decades. Thus, the asphalt industry, road authorities and the related researchers have paid a lot of attention on bitumen modification in order to balance the life-cycle cost and service performance of roads. Among all attempted methods for paving bitumen modification, polymer modification is one of the most popular approaches.

The production of polymer-modified bitumen (PMB) entails a two-phase blend of the bitumen and the polymer modifier. For example, the manufacture of styrene-butadiene-styrene (SBS) modified bitumen starts with adding SBS modifier into the preheated bitumen (usually 180 °C); and then the modifier disperses in the bitumen by low shear stirring or high shear milling, depending on the modifier form (powder or pellet). After dispersion, the polymer swells (or partially dissolves) by absorbing certain components of bitumen. In order to get a well-structured product, stirring may be required during the swelling process. After sufficient swelling of the polymer, quality control tests are carried out and the qualified products are stored for a short term or directly transported to the construction sites. The temperature for short-term storage and transport of SBS-modified bitumen remains the same as the manufacture temperature, usually 180 °C.

As bitumen and polymer modifiers are naturally different and their properties may vary from one source to another, the polymer swelling process and PMB phase behaviour after the swelling may be different

from case to case. Some bitumen and polymer modifiers are quite compatible with each other, so they can lead to the preferred storage-stable PMB products. However, some other combinations may show to have storage instability problem. The separation of polymer from the bitumen during PMB storage and transport is essentially a phase separation process, i.e. the separation of the polymer-rich phase from the bitumen-rich phase.

The phase separation in an unstable PMB is a complex process controlled by many factors. Diffusion and flow may be the main mass transfer modes in this process. In some cases, dynamic asymmetry between the bitumen and polymer may influence the mass transfer processes. Due to the polymer-bitumen density difference, the gravity affects the PMB phase separation in the vertical direction. In the case of crystalline or semicrystalline polymer modifier, e.g. polyethylene (PE) and polypropylene (PP), the polymer crystallization process may become important. With the use of chemically reactive additives (e.g. sulphur), chemical reactions certainly affect the phase separation. Last but not least, the thermal condition, i.e. the temperature level and its changing rate during phase separation, has significant effects on almost every factor mentioned above. Unfortunately, a clear understanding on how these factors affect this complex process has so far still not been sufficiently reached. This today still limits the successful application of PMB and thus reduces some of the potential positive impacts this technology could have on the pavement industry and the road network.

1.2. Aims and Scope

On the basis of the appended scientific articles, this thesis is compiled with its aim at contributing to a *fundamental understanding on PMB storage stability and phase separation behaviour*. In order to reach this aim, the specific research objectives are to:

- Perform a comprehensive and critical state-of-the-art review on polymer modification of paving bitumen;
- Experimentally characterize the phase separation process in PMB and identify the driving forces for the separation;
- Develop a numerical model that is able to predict PMB storage stability and describe the PMB phase separation behaviour;

- Numerically investigate the temperature dependency of PMB phase separation behaviour; and
- Study the coupling between different driving forces for PMB phase separation and its effect on PMB storage stability.

The focus of this thesis is the paving PMB. PMBs for other purposes (e.g. roofing) are out of the scope of this thesis, as they may have different properties compared to the material used for paving of roads. The experiments presented and used for model calibration, as shown in the following chapters, are based on SBS-modified bitumen. But this does not mean that the proposed numerical model is only valid for SBS-modified bitumen. The model has the potential of being applied for other PMBs, as long as all the conditions are fulfilled. Additionally, it is worth mentioning that this thesis concerns the temperature range between 140 °C and 180 °C. Of the investigated temperatures, 180 °C stands for a normal PMB storage temperature; 160 °C corresponds to a lower temperature for long time PMB storage in order to avoid polymer degradation; and 140 °C may help to understand the effect of cooling during the construction process. Within this temperature range, PMB is considered as a pseudo-binary blend.

1.3. Thesis Outline

This thesis consists of seven chapters. After this opening chapter, Chapter 2 gives a comprehensive overview of the development of bitumen polymer modification over the last 40 years. In Chapter 3, fluorescence microscopy is used to observe the morphology of four different SBS-modified bitumen binders and capture the phase separation process in the unstable PMBs at the storage temperature. Chapter 4 describes the development of a phase-field model for storage stability and phase separation behaviour prediction of common PMBs. Chapter 5 numerically investigates the effects of thermal condition on PMB phase separation between 140 °C and 180 °C. Chapter 6 presents a coupled diffusion-flow model and simulates the gravity-driven flow in PMB at the storage temperature. Finally, Chapter 7 summarizes the findings and gives recommendations for future work.

2. State of the Art

This chapter reviews firstly some popular plastomers and thermoplastic elastomers for paving bitumen modification. After that, focus is placed on PMB storage stability and phase separation behaviour.

2.1. Popular Polymers for Bitumen Modification

Before reviewing the popular polymer modifiers, it is worth noting that even for a given polymer modifier, selection of base bitumen still has very important effects on the resulting PMB, as each bitumen has its own particular chemical composition and structure. In addition, base bitumen usually composes over 90% of the PMB by weight, which could introduce overriding influences on the final properties of the PMB.

Bitumen polymer modification has a long history. Even before refined bitumen was produced, people began to modify natural bitumen and some patents were granted for natural rubber modification (Morgan and Mulder, 1995; Isacsson and Lu, 1995; Lewandowski, 1994; Yildirim, 2007). After World War II ended, synthetic polymers began to be used to modify bitumen. Over the years, researchers developed various polymer modifiers. Today, widely used polymers for paving bitumen modification can be classified into two categories: plastomers and thermoplastic elastomers. Some popular polymers for this are listed in Table 2.1 with their advantages and disadvantages.

2.1.1. *Plastomers*

As an important category of plastomers, polyolefin is one of the earliest used modifiers for bitumen. After polyolefin materials are added into bitumen, they are usually swollen by certain components of bitumen. If the polymer content is low, a biphasic structure is formed with a dispersed polyolefin-rich phase in the continuous bitumen-rich matrix.

Table 2.1. Popular polymers for paving bitumen modification.

Categories	Examples	Advantages	Disadvantages
Plastomers	<ul style="list-style-type: none"> Polyethylene (PE) Polypropylene (PP) 	<ul style="list-style-type: none"> Good high-temperature properties Relatively low cost 	<ul style="list-style-type: none"> Limited improvement in elasticity Phase separation problems
	<ul style="list-style-type: none"> Ethylene-vinyl acetate (EVA) Ethylene-butyl acrylate (EBA) 	<ul style="list-style-type: none"> Relatively good storage stability High resistance to rutting 	<ul style="list-style-type: none"> Limited improvement in elastic recovery Limited enhancement in low-temperature properties
Thermoplastic elastomers	<ul style="list-style-type: none"> Styrene-butadiene-styrene (SBS) Styrene-isoprene-styrene (SIS) 	<ul style="list-style-type: none"> Increased stiffness Reduced temperature sensitivity Improved elastic response 	<ul style="list-style-type: none"> Compatibility problems in some bitumen Low resistance to heat, oxidation and ultraviolet Relatively high cost
	<ul style="list-style-type: none"> Styrene-ethylene/butylene-styrene (SEBS) 	<ul style="list-style-type: none"> High resistance to heat, oxidation and ultraviolet 	<ul style="list-style-type: none"> Storage instability problems Relatively reduced elasticity High cost

As the polyolefin concentration increases, phase inversion may occur in some cases. Two interlocked continuous phases are preferable for polyolefin-modified bitumen, which could improve the properties of bitumen to some extent. Those used materials, mainly PE and PP, were usually found to result in high stiffness and good rutting resistance of modified bitumen (Polacco *et al.*, 2005), although they are different in chemical structures as shown in Figure 2.1.

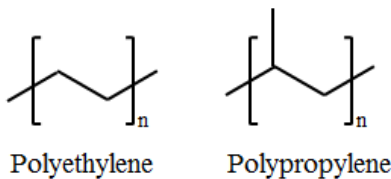


Figure 2.1. Structures of polyethylene (PE) and polypropylene (PP).

However, those used polyolefin materials failed to significantly improve the elasticity of bitumen (Isacsson and Lu, 1995). In addition to this, their regular long chains give them a high tendency to pack closely and crystallize. This could lead to a lack of interaction between the bitumen and polyolefin and result in the instability of the modified bitumen. Furthermore, some researchers claimed that the compatibility of polyolefin with bitumen is very poor because of its non-polar nature (Polacco *et al.*, 2006a). As a result, the limited improvement in elasticity and potential storage stability problems of polyolefin-modified bitumen restrict the application of polyolefin as a paving bitumen modifier, whereas they are popular in production of impermeable membranes.

More popular plastomers in paving bitumen modification are ethylene copolymers, such as ethylene-vinyl acetate (EVA) and ethylene-butyl acrylate (EBA). Due to their similar chemical structures, EVA is discussed here as an example of ethylene copolymers. As seen in Figure 2.2, EVA copolymers are composed of ethylene-vinyl acetate random chains. Compared with PE, the presence of polar acetate groups as short branches in EVA disrupts the closely packed crystalline microstructure of the ethylene-rich segments, reduces the degree of crystallization and increases the polarity of the polymer. This was believed to be beneficial to improving the storage stability of modified bitumen by some researchers (Polacco *et al.*, 2006a). However, the properties of EVA copolymers are closely related to the vinyl acetate content. When the vinyl acetate content

is low, the degree of crystallization is high and the properties of EVA are quite similar to those of low-density polyethylene (LDPE). As the vinyl acetate content increases, EVA tends to present a biphasic microstructure with a stiff PE-like crystalline phase and a rubbery vinyl acetate-rich amorphous phase (Morgan and Mulder, 1995). The higher the vinyl acetate content, the higher the proportion of amorphous phase. But the degree of crystallization should be controlled carefully when EVA is used as a bitumen modifier, because neither too low (getting easy to be disrupted) nor too high (causing the lack of interactions with bitumen) degree of crystallization is good for bitumen modification.

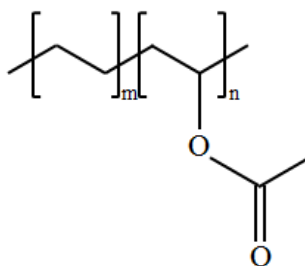


Figure 2.2. Structure of ethylene-vinyl acetate (EVA).

The structure with two interlocked continuous phases is also preferred for EVA-modified bitumen. With such a structure, the binder properties could be improved to a large extent. EVA was found to form a tough and rigid network in the modified bitumen which can help resist deformation (Sengoz *et al.*, 2009). This means that EVA-modified bitumen has an improved resistance to rutting at high temperatures. Although some properties of bitumen are enhanced by EVA modification, there are still some problems limiting its application. One large limitation is the fact that EVA cannot much improve the elastic recovery of bitumen, due to the plastomer nature of EVA (Becker *et al.*, 2001; Isacsson and Lu, 1995).

Furthermore, the glass transition temperature (T_g) of EVA copolymers, which strongly depends on the vinyl acetate content (Stastna *et al.*, 2003), is not low enough to significantly improve the low-temperature properties of bitumen. It was reported that T_g of EVA copolymers with 28.4 wt% of vinyl acetate is -19.9 °C (Champion *et al.*, 2001), which is even quite close to T_g of some base bitumen. As a result, EVA's ability to improve the low-temperature properties of bitumen is rather limited, especially at high

EVA concentrations. According to the research by Ameri *et al.* (2012), bitumen's resistance to low-temperature cracking was increased to some extent by addition of 2 wt% or 4 wt% of EVA, but decreased when adding 6 wt%. In contrast, although EBA could cause potential storage instability of modified bitumen (Isacsson and Lu, 1999), its T_g is much lower than that of EVA with the same content of co-monomer (vinyl acetate or butyl acrylate). It was reported that T_g of EBA copolymers with 33.9 wt% of butyl acrylate is -45.9 °C, which led to the higher cracking resistance of EBA modified bitumen at low temperatures (Champion *et al.*, 2001).

Additionally, the melting temperature of ethylene-rich segments in EVA copolymers is much lower than the usual preparing temperature of modified bitumen. Those rigid crystalline domains could be partially broken by the applied shear forces during the preparation (Polacco *et al.*, 2006a). In order to prepare the ideally modified bitumen by EVA copolymers, the temperature limits for the preparation should be considered (Airey, 2002). Even so, those ethylene-rich segments still could melt and be partially broken by shear when EVA modified bitumen is mixed with mineral aggregates before paving, because the usual mixing temperature is also much higher than the melting temperature of ethylene-rich segments.

2.1.2. Thermoplastic Elastomers

Thermoplastic elastomers are usually more effective than plastomers for paving bitumen modification. The most popular thermoplastic elastomers as paving bitumen modifiers are SBS copolymers and styrene-isoprene-styrene (SIS) copolymers. Due to their similar chemical structures, SBS is discussed here as an example of thermoplastic elastomers. SBS copolymers are composed of styrene-butadiene-styrene triblock chains with a biphasic morphology of dispersed rigid polystyrene (PS) domains in the continuous flexible polybutadiene (PB) matrix, shown as Figure 2.3A. The chemical linkages between PS and PB blocks can immobilize domains in the matrix. T_g of PS blocks is around 95 °C and T_g of PB blocks is around -80 °C (Zanzotto *et al.*, 2000). Under the usual service temperatures of paving bitumen, PS blocks are glassy and contribute to the strength of SBS while PB blocks are rubbery and offer the elasticity (Lucena *et al.*, 2004). Furthermore, the incompatibility between PS and PB blocks makes it possible to physically crosslink PS blocks as uniformly

distributed domains by intermolecular forces at ambient temperatures. This aggregation of PS blocks disappears at high temperatures when the kinetic energy of molecular thermodynamic movements is greater than the energy of intermolecular forces (Zhang *et al.*, 2008). However, as shown in Figure 2.3, the physical crosslinking among PS blocks can be reformed after cooling. The strength and elasticity of SBS can be restored, which is very important for SBS to be a popular bitumen modifier.

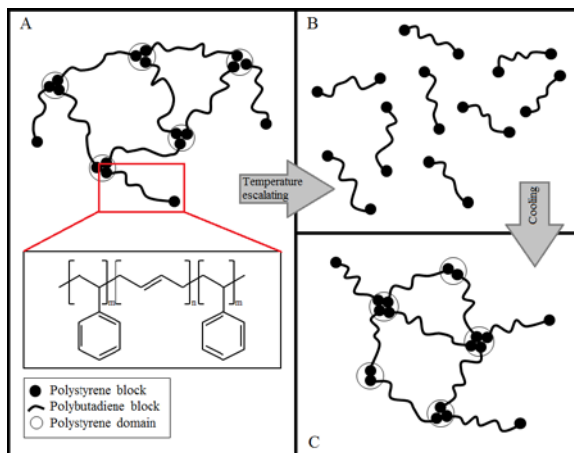


Figure 2.3. Structure of styrene-butadiene-styrene (SBS) copolymer and a schematic illustration of the reversible crosslinks in SBS.

After SBS copolymers are added into bitumen, some interactions happen between bitumen and SBS. Masson *et al.* (2003) reported that intermolecular interactions between bitumen and the PB blocks are stronger than those with the PS blocks. They claimed that PB blocks interact with positively charged groups in bitumen through their π -electrons, whereas PS blocks interact with electron-rich groups in bitumen through their aromatic protons. Mixed with bitumen, PS blocks in SBS copolymers may absorb some saturated branches and a few rings in light components of bitumen (Chen *et al.*, 2002; Airey, 2003), which leads to the swelling of PS blocks and the hardening of bitumen. When the polymer content is low, SBS is dispersed as a discrete phase in the bitumen. As the SBS concentration increases, phase inversion may start in the modified bitumen. It is ideal to form two interlocked continuous phases: bitumen-rich phase and SBS-rich phase. Within the SBS-rich phase, there are two subphases: swollen PB matrix and essentially pure

PS domains. Once the SBS-rich phase forms, a rubbery supporting network is created in the modified bitumen, which results in the increased complex modulus and viscosity, improved elastic response and enhanced cracking resistance at low temperatures of SBS-modified bitumen.

The reported excellent properties, relatively good dispersibility (or appropriate solubility) in bitumen and acceptable cost have made SBS popular as a paving bitumen modifier. However, SBS copolymers are far from an ideal modifier. For example, the compatibility between bitumen and SBS is not that good (Wang *et al.*, 2010; Wen *et al.*, 2002; Galooyak *et al.*, 2010). Airey (2003) claimed that thermoplastic elastomers and asphaltenes compete to absorb the light components of bitumen in SBS-bitumen blends. If these light components are insufficient, phase separation could occur in modified bitumen. It was noted that bitumen with high aromatics content can be helpful in producing compatible and stable SBS-modified bitumen (Kraus, 1982). The addition of aromatic oils can improve the compatibility between SBS and some bitumen with low aromatics content (Masson *et al.*, 2003). Too high aromatics content in modified bitumen, however, may lead to the swelling and antiplasticization of some PS blocks (Włoczyński *et al.*, 1997), which is not good for the final properties of the modified bitumen.

Another problem with SBS modification of paving bitumen is its low resistance to heat, oxidation and ultraviolet (UV) because of the presence of double bonds and α -H in PB blocks (Li *et al.*, 2010; Collins and Bouldin, 1992). In fact, the instability of SBS copolymers is mainly due to the high activity of α -H and low bond energy of the π -bond in double bonds. Undesired chemical reactions (e.g. formation of peroxy radicals and hydroperoxides) make them sensitive to heat, oxidation and UV. In order to overcome this disadvantage, researchers attempted to saturate the thermoplastic elastomer.

Styrene-ethylene/butylene-styrene (SEBS) copolymers, which can be obtained by hydrogenation of SBS, consist of triblock styrene-ethylene/butylene-styrene chains. The chemical saturation makes them highly resistant to heat, oxidation and UV. However, as the double bonds disappear, some researchers claimed that the polarity of the copolymers is considerably reduced (Polacco *et al.*, 2006a). Meanwhile, the ethylene/butylene blocks in SEBS have a trend to crystallize (Vargas *et al.*,

2005). So the compatibility between SEBS and bitumen was believed to become even worse. According to the research by Polacco *et al.* (2006b), stable SEBS-modified bitumen can only be prepared at a low polymer content (below about 4 wt% of the total mass) when SEBS acts just as filler and does not improve the viscoelastic properties of bitumen significantly. On the contrary, when SEBS content is high enough to really modify bitumen, the prepared PMB is unstable and tends to phase separate. Additionally, extra cost involved by the hydrogenation process and poorer elastic properties were observed in SEBS-modified bitumen (Polacco *et al.*, 2006a), which further limits its application as a bitumen modifier.

2.2. PMB Storage Stability and Phase Separation

The previous sections have reviewed the use of some popular polymer modifiers for paving bitumen, including PE, PP, EVA, SBS and SEBS. One of the identified common problems was the storage instability of the final PMB products, that is, the separation of polymer-rich phase from bitumen-rich phase during storage and transport. Since storage stability is a primary requirement for all PMBs, understanding the stability-related behaviour of PMB has always been the interest and focus in this research field during the past decades.

Common methods for characterizing PMB storage stability include the 'tube test' (the European standard EN 13399 and the American ASTM D7173-11) and microscopy observation (Isacsson and Lu, 1995; Polacco *et al.*, 2015). These tests are believed to be reliable, as they directly measure or observe the results caused by the phase separation. But they do not demonstrate the reasons for the separation and will thus not contribute to knowledge that can lead to prevent the problem from occurring.

As mentioned above, the phase separation process in an unstable PMB is controlled by many factors. Among them, the influence of gravity due to polymer-bitumen density difference is believed to be one of the causes for PMB phase separation in the vertical direction (Brûlé, 1996; Giavarini *et al.*, 1996; Ouyang *et al.*, 2005; Pérez-Lepe *et al.*, 2007). Density difference is an important factor for PMB storage stability in the three-dimensional reality, but the gravity effect does not cover all the reasons for PMB phase separation. More significant effects may come from the

bitumen composition, polymer chemistry, polymer content and possibly many other factors (Lu and Isacsson, 1997; Lu *et al.*, 1999; Masson *et al.*, 2003; Sun and Lu, 2006).

By focusing on very thin samples, microscopy is a powerful tool to reduce the dimensions (thus can be used for disregarding the influence of gravity in the vertical direction) and explore the driving forces for the phase separation process in PMB. Many previous studies (Brûlé *et al.*, 1988; Adedeji *et al.*, 1996; Lu and Isacsson, 1997; Lu *et al.*, 1999; Airey, 2002, 2003; Varma *et al.*, 2002; Masson *et al.*, 2003, Hernández *et al.*, 2006; Sun and Lu, 2006; Pérez-Lepe *et al.*, 2007; Sengoz and Isikyakar, 2008a, 2008b; Soenen *et al.*, 2008, 2009; Sengoz *et al.*, 2009; Oliver *et al.*, 2012) employed microscopy to investigate PMB two-dimensional morphology and some tried to understand the relationship of PMB morphology with polymer-bitumen compatibility and PMB storage stability. However, few of these studies have really answered the questions what are the reasons for instability and how the separation happens in an unstable PMB.

Many other studies have focused on the evaluation and prediction of the polymer-bitumen compatibility and thus the PMB storage stability. Some of them (Brûlé *et al.*, 1988; Lu and Isacsson, 1997; Oliver *et al.*, 2012) employed SARA fractions (i.e. saturates, aromatics, resins and asphaltenes) and some derivative compositional parameters. One of the widespread derivative compositional parameters is the so called 'colloidal instability index' I_c , defined as

$$I_c = \frac{\text{Saturates+Asphaltenes}}{\text{Aromatics+ Resins}}. \quad (2.1)$$

It was believed by many that the base bitumen binders with lower asphaltenes content, higher aromatics content or lower I_c value lead to more stable PMB products. However, some researchers (Masson *et al.*, 2003; Polacco *et al.*, 2015) have reported that these criteria can be misleading in some cases. Thus, new criteria still need to be developed. Because of the complex bitumen composition and its wide variety, using only compositional parameters in the criteria might be not enough to show the full picture of polymer-bitumen interaction in PMB. Other aspects should thus also be taken into consideration.

Some other studies (Redelius, 2000, 2004; Cong *et al.*, 2008) have used solubility parameters for the interpretation and prediction of

polymer-bitumen compatibility and PMB storage stability. This theory is based on the fact that solvents with similar solubility parameters as the solute are usually good solvents for the solute. Both the Hildebrand solubility parameter and the Hansen solubility parameters have been discussed in the context of PMB. The latter are believed to provide a better approximation by taking the polar and hydrogen bonding interactions into consideration (Redelius, 2000, 2004). However, the difficulty lies in the indirect determination of solubility parameters (or the solubility body) for bitumen, due to its complex chemical composition.

The Hansen solubility parameters and solubility bodies in the three-dimensional Hansen space are useful tools for analysing the polymer-bitumen compatibility and thus PMB storage stability. However, it is very important to distinguish the solubility body for complete solubility in all concentrations from the space for complete solubility in some limited concentrations, namely partial (incomplete) solubility in the other concentrations. A critical concentration from complete to partial solubility exists for every point outside the all-concentration solubility body in the Hansen space. In the study by Redelius (2004), the construction of the solubility body was actually to find the points (or surface) with the critical concentration the same as the given concentration. Thus, due to the preferred partial solubility of the polymer in bitumen for PMB, a full understanding of polymer-bitumen compatibility has to be based on sufficient solubility data of the bitumen and polymer in sufficient concentrations at different temperatures.

Furthermore, even if sufficient solubility data of the bitumen and polymer have been obtained in the concerned concentrations at the concerned temperatures, the solubility parameters do not give the flux information between the two materials during the dissolution process, i.e. how much of the bitumen goes into the polymer-rich phase and how much of the polymer goes into the bitumen-rich phase. Additionally, solubility parameters by themselves give no indication towards how the two phases form the microstructure (how coarse or fine it is) and how fast (or slow) the dissolution process is. Consequently, more work still needs to be done on solubility parameters of bitumen and polymer modifiers regarding the use for analysing the polymer-bitumen compatibility. At the same time, more approaches to the new criteria for PMB storage stability prediction need to be explored.

3. Experimental Characterization of PMB Storage Stability and Phase Separation

This chapter uses a fluorescence microscopy to observe the morphology of four different SBS-modified bitumen binders at the storage temperature. The morphological results are discussed and compared with the conventional binder test results. Since no separation happens in the stable PMBs, in this chapter, research focus is placed on capturing and analysing the phase separation processes in the unstable PMBs. The discussion leads toward the possibility of having a thermodynamic approach to PMB storage stability and phase behaviour prediction.

3.1. Materials and Method

Four base bitumen binders of different sources were used to prepare PMBs. They were all of penetration grade 70/100 and were numbered as B1, B2, B3 and B4. Their conventional properties are listed in Table 3.1. As for the modifier, a linear triblock SBS copolymer (Kraton® D-1101CU) without silica powder was used. The weight average molecular weight of the SBS copolymer was 189000; the styrene content was about 30%; and the fraction of tri- versus diblock copolymer was 0.8.

Table 3.1. Base bitumen properties.

Sample	B1	B2	B3	B4
Penetration, 25 °C (0.1 mm)	99	93	86	93
Softening point, R&B (°C)	43.0	43.2	43.4	45.5
SARA* fractions (%)	Saturates	8	7	8
	Aromatics	52	55	55
	Resins	20	22	22
	Asphaltenes	20	16	15

* The SARA fractions (i.e. saturates, aromatics, resins and asphaltenes) were determined using thin-layer chromatography with flame ionization detection (TLC-FID).

Four PMBs were prepared by respectively mixing 5% SBS copolymer (by weight of the blend) with the four base bitumen binders at 180 °C, numbered as PMB1, PMB2, PMB3 and PMB4 accordingly. Stirring at about 500 rpm was applied for 3 hours during the preparation. After preparation, some conventional binder tests were carried out for all the four PMBs, including the penetration and softening point tests. Tube test for assessing PMB storage stability was conducted according to the Standard EN 13399. A summation of the test results is shown in Table 3.2.

Table 3.2. Polymer-modified bitumen properties.

Sample	PMB1	PMB2	PMB3	PMB4
Penetration, 25 °C (0.1 mm)	57	52	56	52
Softening point, R&B (°C)	76.0	85.0	77.8	65.0
Storage stability tube test, R&B (°C)	Top	94.5	86.5	54.6
	Bottom	69.0	86.5	55.6
	Difference	25.5	0.0	-1.0
				32.0

Because SBS copolymer and bitumen naturally have different UV excitation responses, the SBS-rich phase exhibits higher fluorescence than the bitumen-rich phase when observed with a fluorescence microscope. Thus, the SBS-rich phase appears much lighter than the bitumen-rich phase under a fluorescence microscope. In this research, an Olympus® BX51 fluorescence microscope with a Leica® DC300 camera was used to observe the PMB morphology and capture the phase separation process. The ‘thin film method’ (Soenen *et al.*, 2008) was used for sample preparation.

The experiment was to observe the morphology of the four PMBs at the storage temperature (180 °C) and capture the phase separation process in the unstable PMBs. Since those unstable samples had already shown separation at 180 °C (PMB1 and PMB4 in this study), in order to see how the phase separation actually happened from a well-dispersed ‘one-phase’ state, the drops of PMB1 and PMB4 were taken from an increased temperature, i.e. 200 °C. Drops of PMB2 and PMB3 were taken from 180 °C. After the preparation of thin film samples for the four PMBs, all the microscope slides were divided into five groups for isothermal annealing conditioning. The conditioning was conducted at 180 °C with different conditioning time: one group without conditioning and four

groups respectively for 5 min, 10 min, 30 min and 60 min. After the isothermal annealing conditioning, the slides were left on a conductive holder for cooling to the ambient temperature. In order to minimize the orientation effects because of sample flowing during the spreading and conditioning, the observation was focusing on the possibly original drop centre areas of the slides. The procedure of fluorescence microscopy observation is shown in Figure 3.1.

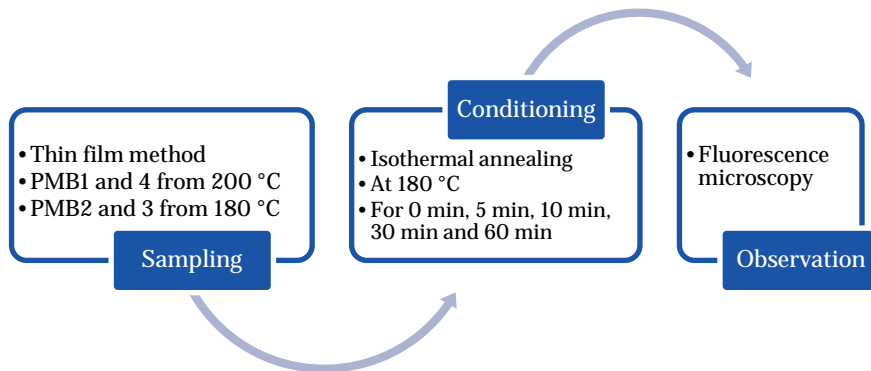


Figure 3.1. Procedure of fluorescence microscopy observation.

3.2. Experimental Results and Analysis

Fluorescence microscopy images of the four PMBs during the isothermal annealing conditioning are shown in Figures 3.2-3.4. It can be seen that PMB2 and PMB3 remained stable along the time, while PMB1 and PMB4 separated into two phases. This can be correlated with the PMB tube test results in Table 3.2. Since the whole processes after the initial states have been observed in two dimensions, it would be interesting to see the absence of gravity effect in the experiment. As the gravity influence due to polymer-bitumen density difference is an important factor for the tube test but not necessarily for the microscopy observation, the correlation between the results can lead to the hypothesis that the gravity influence does not directly cause but accelerates the possible phase separation in the vertical direction. This means that an unstable PMB starts to separate into two phases because of the poor polymer-bitumen compatibility. Once the two phases form sufficiently big density difference, gravity starts to play the role and accelerate the separation in the vertical direction.

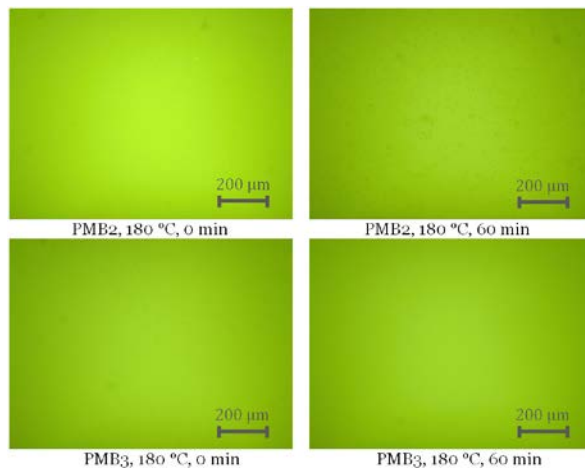


Figure 3.2. Fluorescence microscopy images of PMB2 and PMB3 before and after isothermal annealing conditioning at 180 °C.

Figure 3.2 shows the fluorescence microscopy images of PMB2 and PMB3 before and after isothermal annealing conditioning at 180 °C for 60 min. It can be seen from the images that PMB2 and PMB3 were still homogeneous at this scale after isothermal annealing. This was also the case for each sample of any other conditioning time between 0 and 60 min. This means that PMB2 and PMB3 are stable even after some time of high-temperature storage. Since no separation happened in the stable PMB2 and PMB3, in order to identify the driving forces for PMB phase separation and prevent the instability problem from occurring, further focus is placed on capturing and investigating the phase separation process in PMB1 and PMB4.

The captured phase separation processes in PMB1 and PMB4 during isothermal annealing conditioning at 180 °C are respectively shown in Figure 3.3 and Figure 3.4. From Figure 3.3, it can be seen that PMB1 became homogeneous at 200 °C at this magnification level. During the isothermal annealing conditioning at 180 °C, PMB1 separated into a SBS-rich phase and a bitumen-rich phase. The SBS-rich phase in PMB1 was continuous in the beginning stage. However, as the separation process continued, the network of SBS-rich phase broke down and the SBS-rich phase became dispersed after 60 min. In contrast, the bitumen-rich phase in PMB1 formed isolated droplets in the beginning but finally became a continuous matrix. This is a typical phase inversion phenomenon.

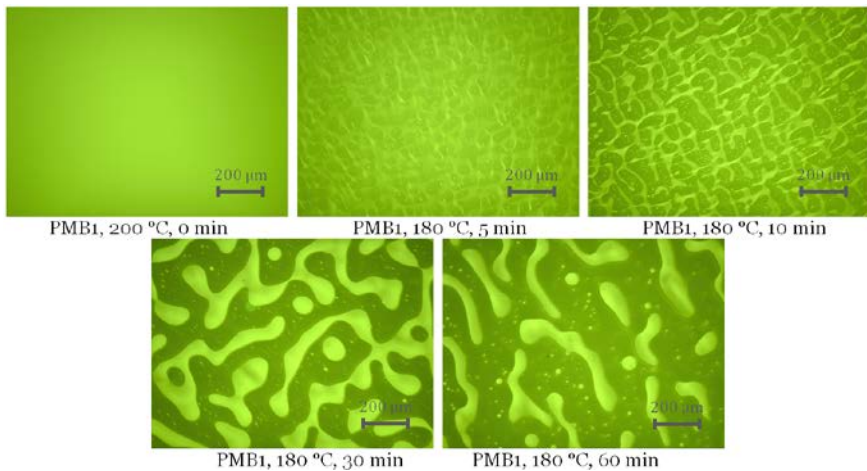


Figure 3.3. Phase separation process in PMB1 during isothermal annealing conditioning at 180 °C. The lighter phase is SBS-rich phase; and the darker phase is bitumen-rich phase.

Phase inversion is one main feature of viscoelastic phase separation in binary blends. It may happen in some PMBs. This is an inversion process that happens over time in one single PMB sample. Some previous studies (Airey, 2002; Sengoz and Isikyakar, 2008a; Sengoz *et al.*, 2009) also reported another phase inversion phenomenon in PMB, which is an inversion process with increasing polymer content in different PMB samples. It is important to distinguish these two phenomena, as they may have similar names but are different physical concepts. Here in this chapter, the phase inversion is due to the dynamic asymmetry between bitumen and polymer. This dynamic asymmetry can also lead to another feature of viscoelastic phase separation, i.e. volume shrinking of the slow phase. This study is currently not focusing on it and will leave it for future investigations. However, Figure 3.3 has shown the possible viscoelastic effects on PMB phase separation. Some other researchers also reported the same conclusion by presenting their own experimental results in a recent publication (Xia *et al.*, 2016). Therefore, the dynamic asymmetry between bitumen and polymer may affect the PMB phase separation in some cases.

From Figure 3.4, it can be seen that PMB4 still showed a binary structure at 200 °C, with SBS-rich droplets in a continuous bitumen-rich matrix. During the isothermal annealing conditioning at 180 °C, the SBS-

rich droplets became coarsened but always kept dispersed. One very interesting question arises here: Why do PMB1 and PMB4 show different patterns on their fluorescence microscopy images, both made with the same polymer content by weight? The most plausible answer is the different materials used to prepare the PMBs, i.e. the different base bitumen binders. As mentioned in the previous section, polymer modifiers usually experience a swelling process during PMB production. Even for one single polymer modifier, different base bitumen binders can result in different swelling ratios of the polymer, depending on the base bitumen composition and its molecular chemistry. Different swelling ratios can lead to different volume fractions and concentrations of the equilibrium phases. In order to explicitly describe this process, it becomes critical to understand the thermodynamics of PMB phase separation.

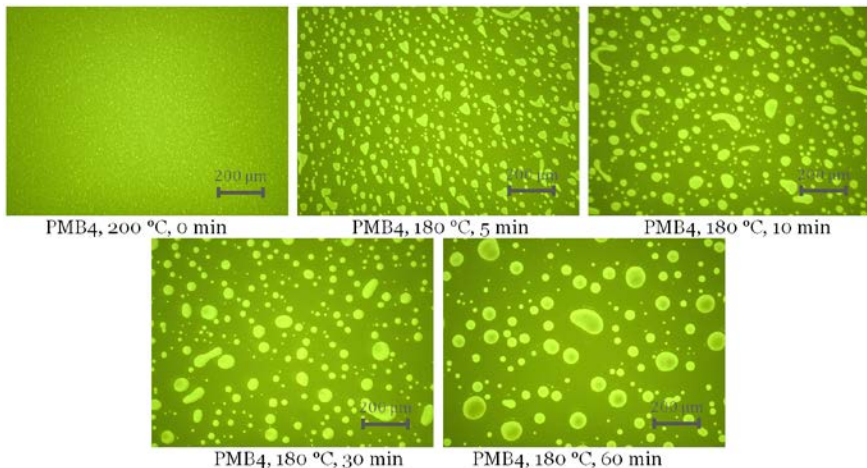


Figure 3.4. Phase separation process in PMB4 during isothermal annealing conditioning at 180 °C. The lighter phase is SBS-rich phase; and the darker phase is bitumen-rich phase.

3.3. Thermodynamics of PMB Phase Separation

As a potential approach to the new criteria for PMB storage stability prediction, understanding the equilibrium thermodynamics and phase separation dynamics of PMB relies on analysing the free energy of PMB system and the related parameters. The classic Flory-Huggins theory (Flory, 1942, 1953; Huggins, 1942a, 1942b) provides a possibility to look

into the free energy of PMB as a pseudo-binary blend. The theory originally uses a simple expression for the molar free energy of mixing of a binary polymer blend, i.e.

$$\Delta f_m = RT \left[\frac{\phi_1}{N_1} \ln(\phi_1) + \frac{\phi_2}{N_2} \ln(\phi_2) + \phi_1 \phi_2 \chi \right], \quad (3.1)$$

where Δf_m is the molar free energy of mixing of the blend (per mole of segments); R is the universal gas constant; T is the temperature; ϕ_1 and ϕ_2 are local volume fractions of the two polymers; χ is the interaction parameter between the two polymers; N_1 and N_2 are segment numbers of the two polymer chains in the Flory-Huggins lattice. The parameters N_1 and N_2 , showing the size of the polymer chains, are not necessarily equal to but proportional to the degree of polymerization and molecular weight of the polymers. The interaction parameter χ characterizes the degree of interaction between the two polymers and can be calculated with the Hansen solubility parameters of the two polymers (Painter, 1993; Lindvig *et al.*, 2002; Emerson *et al.*, 2013) by

$$\chi = \frac{V_s}{RT} \left[(\delta_{D1} - \delta_{D2})^2 + \frac{(\delta_{P1} - \delta_{P2})^2}{4} + \frac{(\delta_{H1} - \delta_{H2})^2}{4} \right], \quad (3.2)$$

where V_s is the molar volume of the segments in the Flory-Huggins lattice; δ_D , δ_P and δ_H are respectively the dispersion, polar and hydrogen bonding components of the Hansen solubility parameters of the two polymers (subscripts 1 and 2). It is worth mentioning that the Flory-Huggins theory assumes weak interactions (dispersion and weak polar forces) for the polymers and Equation 3.2 gives good approximations only when the weak interactions is dominant in the blend. The results from Redelius (2000, 2004) indicated that the dispersion component of bitumen solubility parameters is much larger than the polar and hydrogen bonding components. This confirms the possibility of using Flory-Huggins theory and Equation 3.2 in the context of PMB.

However, as the major component of PMB, bitumen is not a polymeric material but a complex mixture consisting of a continuum of relatively large hydrocarbons (Redelius and Soenen, 2015). According to a report (Painter, 1993) by the American Strategic Highway Research Program (SHRP-A-675), when applying the Flory-Huggins theory for bitumen, simplification can be made by assuming bitumen as hypothetical chains of average segments. In this regard, the hypothetical chains will have an

equivalent molecular weight that is different with the actual parameter of the bitumen.

For simplicity, we assume $N_1=N_2=N$ for a PMB here (subscript 1 for the polymer and 2 for the bitumen), which is not necessarily true for all PMBs but just a convenience here. Under the incompressible condition, we have $\phi_2=1-\phi_1$. Although no available solubility data has been found for PMB at the storage temperature, it is believed that the value of $N\chi$ depends on the temperature and the chemical nature of the bitumen and polymer. It has the theoretical range where $N\chi \leq 2.0$ results in a single-well potential and $N\chi > 2.0$ leads to a double-well potential (Tanaka and Araki, 1997; Araki and Tanaka, 2001; Zhou *et al.*, 2006; Kringos *et al.*, 2011). Defining ϕ as the local volume fraction of the polymer in PMB, Figure 3.5 shows results of the molar free energy of mixing of the PMB (per mole of chains) at 180 °C (453.15 K) with different $N\chi$ values.

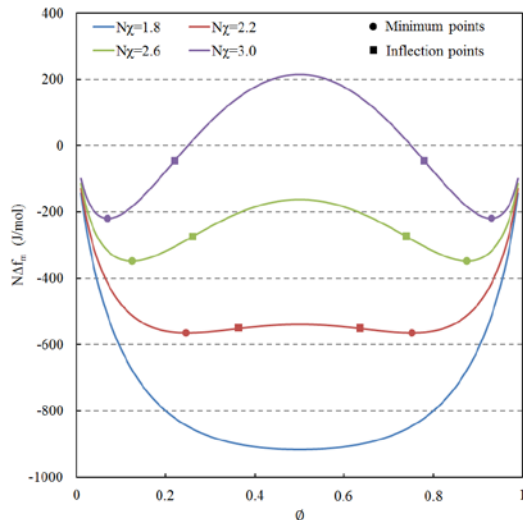


Figure 3.5. Flory-Huggins free energy of mixing of PMB at 180 °C.

When the solubility parameter difference between the polymer and bitumen is small, the $N\chi$ value can be less than 2.0. It is indicated in Figure 3.5 that the free energy of mixing is a single well with $N\chi=1.8$. In this case, the polymer is completely soluble in bitumen in all concentrations. But this case is rare and not a preferred case for PMB in reality. As the difference between the polymer and bitumen in solubility

parameters becomes larger ($N\chi > 2.0$), the free energy of mixing forms a double well which has two minimum points (the dots in Figure 3.5) and two inflection points (the squares in Figure 3.5). The minimum points decide the composition of the equilibrium phases (one for the bitumen-rich phase and the other for the polymer-rich phase), as they are the optimum and end of the free energy minimization. Thus, the location of binodal points at that temperature can be determined on the phase diagram. When the same has been done at different temperatures, the binodal curve of the PMB then can be plotted on its phase diagram. In addition, the spinodal curve can be constructed by plotting the inflection points at different temperatures. In this regard, the portion between the two inflection points of a double-well free energy curve represents the unstable state of the blend; the portions between a minimum point and an inflection point mean the metastable state; and the portions beyond the minimum points indicate the one-phase state. It is also can be seen from Figure 3.5 that, as the $N\chi$ value increases from 2.2 to 3.0 (which means that the solubility parameter difference enlarges), the interval for the unstable state becomes larger and the intervals for the one-phase state become smaller.

Nevertheless, the Flory-Huggins theory is an approximation theory which has its limitations. As a consequence, we can see in Figure 3.5 that the discussed minimum points and inflection points locate on both sides with respect to $\phi=0.5$. This cannot represent the fact that the polymer modifier swells significantly in PMB (the swelling ratio can be up to nine according to Sengoz and Isikyakar (2008a)). The reason for the polymer swelling in PMB is that the bitumen molecules that go into the polymer-rich phase from the bitumen-rich phase are much more than the polymer chains that go into the bitumen-rich phase from the polymer-rich phase. According to the experimental measurement results from Mouillet *et al.* (2008), the local fraction of the polymer in the bitumen-rich phase of a common PMB (modified with SBS and ethylene-vinyl acetate, polymer content 6% in the study by Mouillet *et al.* (2008)) is usually less than 1%, while the local polymer fraction may range from around 7% to around 12% in the polymer-rich phase. This means the minimum points and inflection points of the free energy curve of a common PMB usually lie in the very beginning portion of the ϕ axis, if defining ϕ as the local volume fraction of the polymer in the PMB. More discussion is presented in the next chapter for appropriately expressing the free energy of PMBs.

4. Phase-Field Modelling of PMB Phase Separation at Storage Temperature

Based on the experimental results and discussion in the previous chapter, this chapter continues the exploration of a thermodynamic approach and describes the development of a phase-field model for storage stability and phase separation behaviour prediction of common PMBs. The expression of free energy for PMB system is discussed on the basis of the Flory-Huggins theory. Following the model development, numerical simulation results are analysed under various conditions, in order to separately identify the influence of every involved model parameter.

4.1. Phase-Field Model for PMB Phase Separation

Since the effects of flow were minimized in the experimental study described above, this chapter further explores a diffusion model based on the Cahn-Hilliard equation, i.e.

$$\frac{\partial \phi}{\partial t} = \nabla \cdot M(\phi) \nabla \frac{\delta F}{\delta \phi}, \quad (4.1)$$

where ϕ is the local volume fraction of polymer in PMB; t is the time; $M(\phi)$ is the mobility coefficient of the phase; and F is the free energy of the PMB system. The viscoelastic effects due to the dynamic asymmetry between bitumen and polymer are represented in this chapter by introducing an ϕ -dependent phase mobility coefficient $M(\phi)$. Under the incompressible condition, a linear dependency of the mobility coefficients of the polymer and bitumen, M_p and M_b respectively, is postulated as

$$M(\phi) = M_p \phi + M_b (1 - \phi). \quad (4.2)$$

Besides the dependency of the mobility coefficient on the local composition, the only variable that needs to be determined is the free energy of the PMB system. It introduces the thermodynamic effects into the model.

The expression of the free energy for PMB system has to be based on the fact that bitumen is a complex mixture of various molecules. Bitumen composition and its molecular chemistry certainly have very strong influences on the free energy of PMB system. Since this chapter is considering storage stability prediction of common road paving PMBs, the discussed temperature level is fixed and quite high, e.g. usually around 180 °C for SBS-modified bitumen. At such a high temperature, there is actually no coherent microstructure formed in the PMB. Consequently, elastic energy (usually generated during solid-solid phase transformation) is not involved in this case (Hu and Chen, 2001; Zhu *et al.*, 2001). Neither are other forms of long-range free energy. In this regard, the free energy F of a PMB system consists of the local free energy (its density as f_{loc}) and the gradient energy (its density as f_{gr}), such that

$$F = \int_V (f_{loc} + f_{gr}) dV. \quad (4.3)$$

where V is the volume of the considered body. The common expression of the gradient energy density f_{gr} (Chen, 2002; Moelans *et al.*, 2008; Tanaka and Araki, 1997; Araki and Tanaka, 2001; Ubachs *et al.*, 2004; Zhou *et al.*, 2006), given by

$$f_{gr} = \frac{1}{2} \kappa |\nabla \phi|^2, \quad (4.4)$$

is used in the model. In Equation 4.4, κ is the gradient energy coefficient.

Considering PMB as a pseudo-binary blend, the local free energy of the system includes the free energy of pure polymer and bitumen as well as the free energy change due to mixing the two components, i.e.

$$f_{loc} = f_0 + \Delta f_m, \quad (4.5)$$

where f_0 is the free energy density of pure components (sum of polymer and bitumen) and Δf_m is the free energy density change due to mixing. For a given blend, the free energy of the pure components keeps constant at a fixed temperature. The free energy of mixing can be represented by a double-well potential on the basis of the above discussed Flory-Huggins free energy of mixing.

However, the Flory-Huggins theory is an approximation theory for which a lattice is used and some simplifying assumptions are made. In order to determine the appropriate expression of the free energy for PMB, certain simplifications must be made for the PMB system accordingly. The common polymer modifiers used in PMB are industrially synthesized

products where branching usually happens during the synthesis. In order to hypothesize a lattice for PMB, all the polymer chains are simplified into straight chains. In the case of copolymer, different structural units exist in the polymer chains. A hypothetical lattice for SBS-modified bitumen is shown in Figure 4.2A. However, further approximation based on molar volume (or molecular weight) of the SBS copolymers still needs to be made to have hypothetical chains with single segment size like in the lattice for polymer blends (Figure 4.2B).

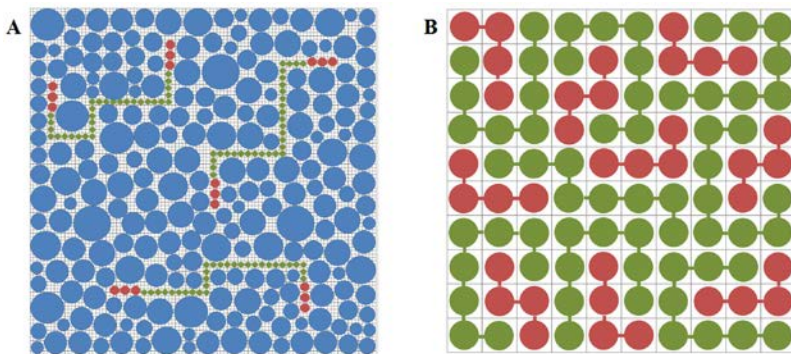


Figure 4.2. (A) Hypothetical lattice for SBS-modified bitumen. Blue=bitumen; red=polystyrene blocks in SBS; and green=polybutadiene blocks. (B) Flory-Huggins lattice for polymer blends. The red and green colours represent different polymers.

Bitumen, the other component in PMB, is a complex mixture consisting of a continuum of relatively large hydrocarbons. The hydrocarbons are different in size, polarity and aromaticity. The exact range of molecular size varies from case to case, depending on the production process and crude oil source. But it is estimated that the size of hydrocarbons in bitumen may range from 20 up to 110 carbons (Redelius and Soenen, 2015). In order to hypothesize a lattice for PMB, the molecules in bitumen are simplified into molecules of different sizes, as indicated in Figure 4.2A. It can be seen that PMB is neither a typical polymer solution case nor a typical polymer blend case.

Furthermore, because of the property diversity, it is not reasonable to simply approximate the bitumen molecules into molecules of the average size. However, due to the size and chemistry diversity of bitumen molecules, configurational entropy can arise from the variety of ways of

arranging the bitumen molecules in the lattice, which has similar effects as the arrangement of the polymer chains. Thus, it is believed that the bitumen molecules in Figure 4.2A can be further approximated into hypothetical chains with single segment size like in the lattice for polymer blends (Figure 4.2B). In this regard, the hypothetical chains will have an equivalent molar volume (and equivalent molecular weight) that is different with the actual parameter of the bitumen.

Additionally, the Flory-Huggins theory does not properly describe the swelling of polymer in PMB. This theory gives good approximations on the fluxes of the two phases only when the polymer content of the PMB is sufficiently high. Due to the complex composition of bitumen, in a given PMB, the bitumen molecules might show a continuum of χ values with the polymer. Some of the molecules may be very interactive with the polymer, while some others may be not interactive at all. The polymer swells by absorbing the interactive molecules of bitumen, but it is just very few polymer chains that go into the bitumen-rich phase. The extent of polymer swelling thus depends on the amount of interactive molecules in the bitumen. In this regard, for describing the interaction between polymer and the hypothetical chain of bitumen, the amount of interactive molecules in bitumen becomes as important as the degree of interaction between polymer and these interactive molecules.

Consequently, a new parameter, named dilution parameter in this thesis, is introduced into the model as a simplification for taking the influence of the interactive molecules amount into account. The meaning of this parameter can be interpreted by a hypothetical dilution process. Some previous investigations (Brûlé *et al.*, 1988; Fuentes-Audén *et al.*, 2008) have observed that the swelling ratio of the polymer in PMB decreases when the polymer content increases, lightly or sharply depending on the material properties and discussed range of polymer content. Within the practical range of polymer content in PMB, the swelling ratio is relatively high and can be up to nine (Sengoz and Isikyakar, 2008a). The assumption is to take a representative part of the bitumen like one column of cells in Figure 4.3, which has the same composition as the original bitumen, to achieve the high-polymer-content interaction between polymer and the hypothetical chain of bitumen assumed by the Flory-Huggins theory with respect to a representative χ value. At this moment, the blend represents the case with sufficiently high polymer content. After this, all the other parts of the bitumen (i.e. all the

other cells in Figure 4.3) are supposed to dilute the blend as a simplification for polymer swelling. As the relative amount of interactive molecules in bitumen decides how much the representative part is, the dilution parameter can thus reflect the influence of the interactive molecules amount in bitumen. In this sense, it is a parameter which depends on the temperature and the local composition.

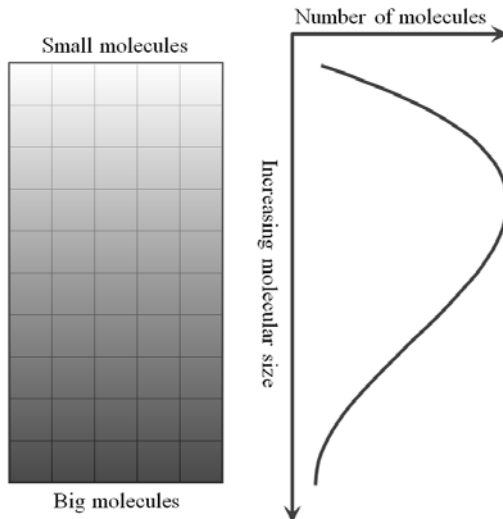


Figure 4.3. The dilution assumption for simplifying the modelled PMB phase separation process. Each cell in the figure may represent different amounts of molecules in the bitumen.

Based on the above discussion, defining \emptyset as the local volume fraction of the polymer in PMB and under the incompressible condition, the proposed free energy density of mixing for PMB can be expressed by

$$\Delta f_m = RT \left[\frac{z\emptyset}{N_p} \ln(z\emptyset) + \frac{1-z\emptyset}{N_b} \ln(1-z\emptyset) + z\emptyset(1-z\emptyset)\chi \right], \quad (4.6)$$

where N_p is the segment number of the polymer chain; N_b is the segment number of the hypothetical chain for bitumen; and z is the dilution parameter. In the equation, N_p and N_b characterize the molecular size (and its distribution for bitumen) of the polymer and bitumen; χ characterizes the degree of interaction between polymer and bitumen; and z characterizes the relative amount of interactive molecules in the bitumen. It is worth mentioning that the dilution parameter z actually includes the effects of polymer content in PMB.

4.2. Model Implementation and Parametric Studies

The model described in the previous section has been implemented in the finite element software COMSOL Multiphysics®. The numerical simulations are performed on a rectangular domain of $1.2 \text{ mm} \times 0.9 \text{ mm}$ meshed with triangular elements. This domain is basically the same size as the microscopic images obtained in Chapter 3. Boundary conditions are set by having a contact angle of 90° on the four sides of the rectangle. Initial values are generated by a normally distributed random function with a mean value of 0.05 and a standard deviation of 0.005, as presented in Figure 4.4. This means that the polymer content in the simulated PMB is 5% by weight with certain variation, if neglecting the density difference between the polymer and bitumen. It can be seen from Figure 4.4 that the local polymer volume fraction in the PMB can range from 3.11×10^{-2} up to 7.13×10^{-2} , which is believed to represent the actual initial condition of a real PMB. Within the limits, the specific range may vary from case to case depending on the parameters.

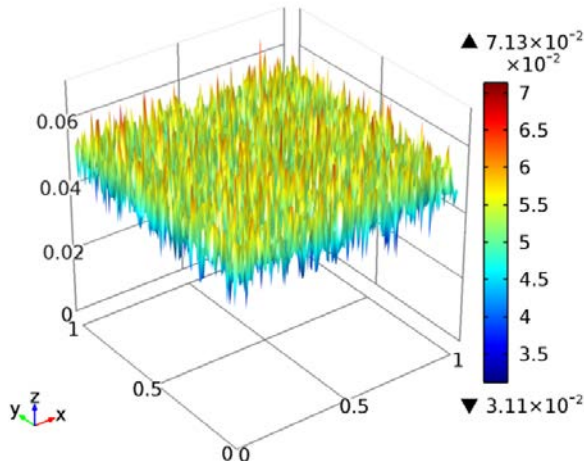


Figure 4.4. The normally distributed random function with a mean value of 0.05 and a standard deviation of 0.005.

For the model implementation, the mobility coefficients (M_p and M_b), gradient energy coefficient κ , segment numbers of the chains (N_p and N_b), interaction parameter χ and dilution parameter z are needed. Theoretically, the mobility coefficient $M(\phi)$ is a variable related to the

interdiffusion (or chemical diffusion) coefficient $D(\emptyset)$ between the two components (Moelans *et al.*, 2008). If sufficient information is available, $M(\emptyset)$ can be determined by: 1) experimental measurements of the diffusion coefficients or 2) theoretical calculation with the atomic mobility coefficients of the constituting elements. As diffusion coefficient measurements are still not performed very commonly for PMBs and there is still a lack of related thermodynamic and chemical information, this chapter uses values of M_p and M_b to determine $M(\emptyset)$ (Equation 4.2), instead of direct determination.

The gradient energy coefficient κ is a positive parameter related to the interfacial tension and thickness between the phases (if more than one phase). Considering the length scale of the interfaces, κ can only be determined by interactive procedures between computational models and available experimental characterization techniques (Kringos *et al.*, 2011), which have not been widely reported or studied for PMBs. Due to the lack of available data for PMBs, the used values of M_p , M_b and κ in this chapter, representing various conditions, are obtained by preliminary estimation based on the reported values for general models and other materials like polymer blends and alloys (Ubachs *et al.*, 2004; Badalassi *et al.*, 2003; Anders and Weinberg, 2012; Anders *et al.*, 2012).

For all the simulations in this chapter, the universal gas constant R equals to 8.314 J/(mol·K) and the temperature is constant at 180 °C (453.15 K). For N_p and N_b , it is postulated that the hypothetical chains for bitumen have the same length as the polymer chains. This does not mean that the bitumen has the same molecular size as the polymer chains. But the complexity of bitumen composition, due to its diversity in chemical species, has the same contribution to the configurational entropy as the polymer chains. In other words, N_b is not the actual value of the bitumen molecular weight but a parameter representing the complexity of the bitumen composition.

In this regard, Equation 4.6 can be reduced into a simple mathematical form by setting $N_p = N_b = N$ without affecting the minimization of the free energy. Thus, $N\chi$ also accordingly scales up into the widely reported theoretical range where $N\chi \leq 2.0$ results in a single well and $N\chi > 2.0$ leads to a double well, as discussed in the previous chapter. About the dilution parameter z , the values can be preliminarily estimated based on the reported swelling ratio values of polymer in PMB. According to the measurement results by Brûlé *et al.* (1988), Fuentes-

Audén *et al.* (2008), and Sengoz and Isikyakar (2008a), it is believed that z may range from 5.0 to 9.0 in most cases within the practical range of polymer content in PMB. In order to show the influence of each involved parameter, parametric studies are conducted with the estimated values shown in Table 4.1. In Table 4.1, Cases 4.1-4.3 are intended for studying the effects of the mobility and gradient energy coefficients, Cases 4.4-4.6 together with Case 4.1 for studying the interaction and dilution parameters, and Cases 4.7-4.9 for stable systems. A constant N value is assumed for all these cases. The change of $N\chi$ thus reflects the change of the interaction parameter χ here. In addition, the independency between M_p and M_b is hereby not investigated in the parametric study cases. This means that M_p and M_b always varies with the same rate between the cases in this chapter, instead of individual rates.

Table 4.1. Parametric study cases.

Cases	M_p [$\text{m}^5/(\text{J}\cdot\text{s})$]	M_b [$\text{m}^5/(\text{J}\cdot\text{s})$]	κ [J/m]	$N\chi$	z
4.1	6.00×10^{-18}	1.80×10^{-17}	4.50×10^{-5}	2.9	8.7
4.2	2.25×10^{-18}	6.75×10^{-18}	4.50×10^{-5}	2.9	8.7
4.3	6.00×10^{-18}	1.80×10^{-17}	9.00×10^{-6}	2.9	8.7
4.4	6.00×10^{-18}	1.80×10^{-17}	4.50×10^{-5}	3.6	8.7
4.5	6.00×10^{-18}	1.80×10^{-17}	4.50×10^{-5}	2.9	7.0
4.6	6.00×10^{-18}	1.80×10^{-17}	4.50×10^{-5}	3.6	7.0
4.7	2.40×10^{-21}	7.20×10^{-21}	9.00×10^{-7}	2.9	8.7
4.8	6.00×10^{-18}	1.80×10^{-17}	4.50×10^{-5}	1.9	7.0
4.9	6.00×10^{-18}	1.80×10^{-17}	4.50×10^{-5}	2.1	9.0

Parametric study results on the mobility coefficients (M_p and M_b) and gradient energy coefficient κ are shown in Figure 4.5. The effect of mobility coefficients can be seen by comparing Case 4.1 and Case 4.2. Because Case 4.2 has lower mobility coefficients than Case 4.1, the phase separation process occurs more slowly in Case 4.2. It is noticed that the result at 1800 s in Case 4.2 is quite similar as the result at 600 s in Case 4.1. Thus, Case 4.2 allows us to look into the early stage of a fast separation. In Case 4.2, the polymer-rich phase (warmer colours) is continuous at 300 s. As the separation process continues, the polymer-rich phase becomes dispersed and coarsens. Since it is only very slight dynamic asymmetry between bitumen and polymer that is introduced into the model, this phase inversion phenomenon may be just partially due to the ϕ -dependent mobility coefficient. However, more research still

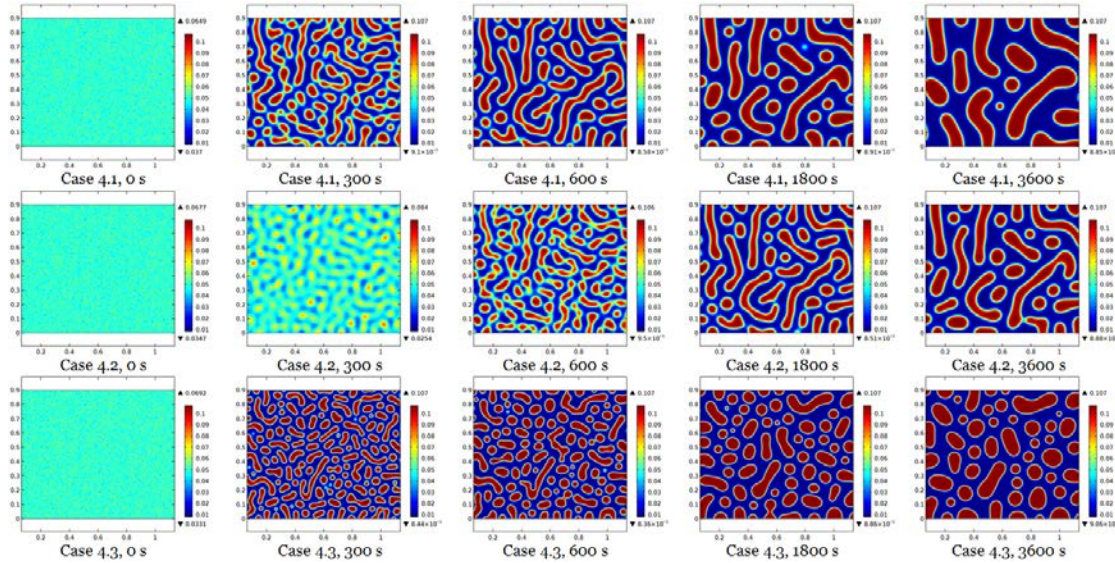


Figure 4.5. Parametric study results on the mobility coefficients and gradient energy coefficient κ .

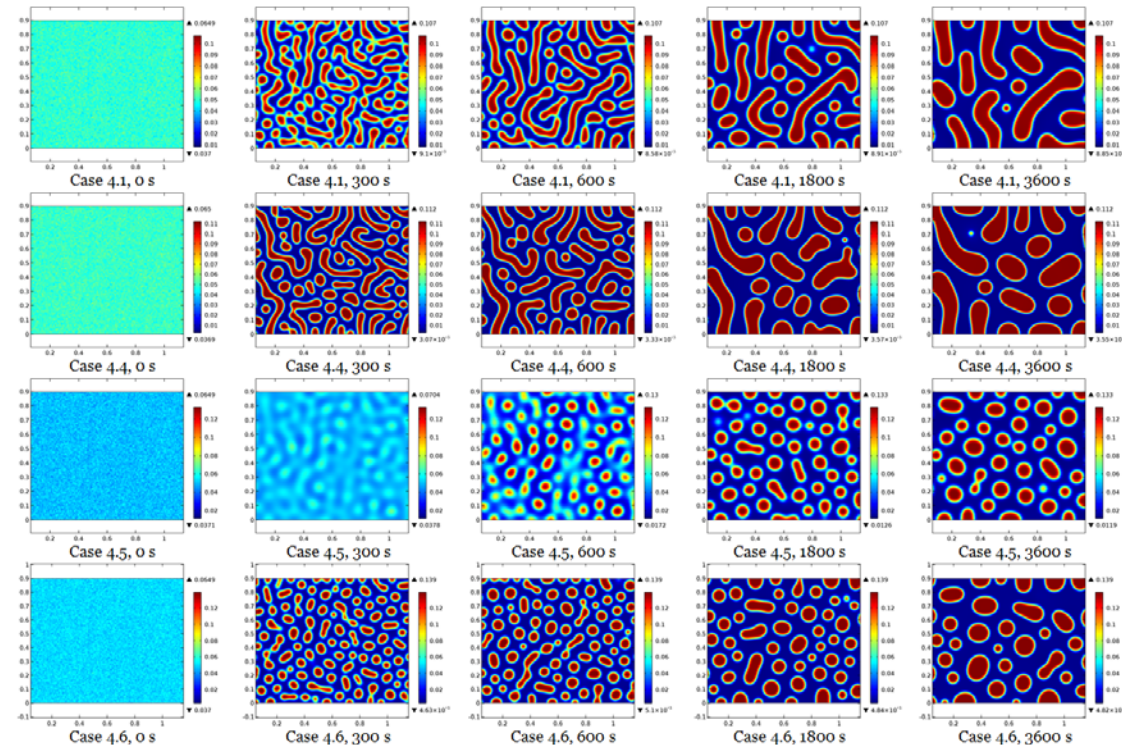


Figure 4.6. Parametric study results on the interaction parameter χ and dilution parameter z .

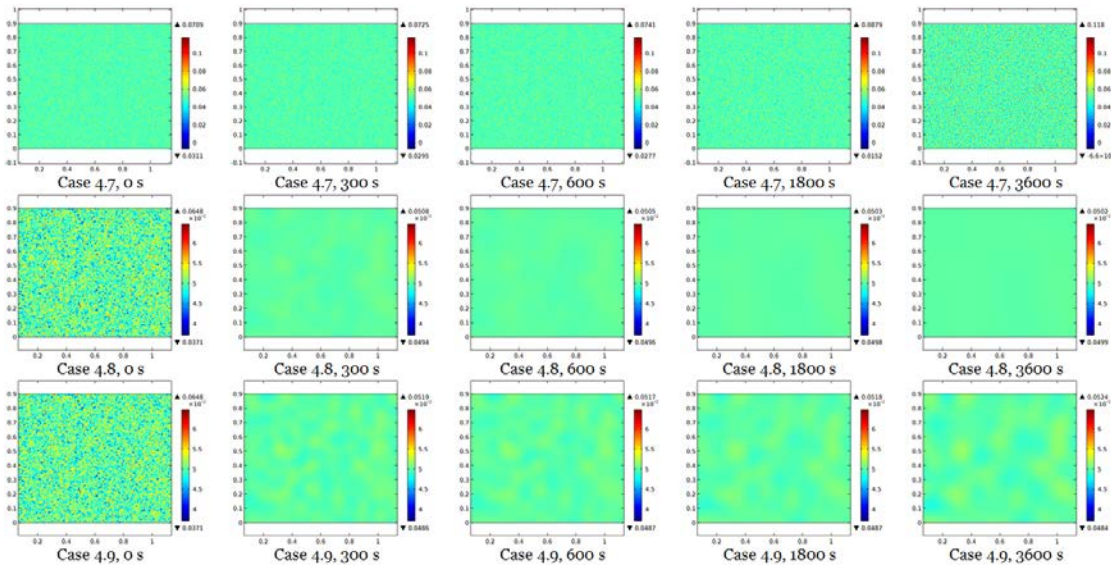


Figure 4.7. Parametric study results on the stable cases.

needs to be done for understanding and incorporating strong viscoelastic effects in the model. The inversion process also happens in Case 4.1 before 300 s. Furthermore, the implication of gradient energy coefficient κ can be seen by comparing Case 4.1 and Case 4.3. With a lower gradient energy coefficient, Case 4.3 displays a finer structure and sharper interfaces than Case 4.1. Controlled by the $N\chi$ value and dilution parameter z , the equilibrium phase composition (polymer volume fraction) of all the three cases in Figure 4.5 keeps the same, i.e. 10.7% for polymer-rich phase and around 0.9% for bitumen-rich phase. This simulation result agrees well with the experimental measurement results by Mouillet *et al.* (2008).

Assuming a constant N value for all cases, parametric study results on the interaction parameter χ and dilution parameter z are shown in Figure 4.6. As χ reflects the energy change due to mixing and z characterizes the relative amount of interactive molecules in the bitumen, a lower χ value (i.e. lower energy change and easier interaction) indicates a higher degree of interaction between the polymer and bitumen and a higher z value means the relative amount of interactive molecules in the bitumen is higher. Thus, Case 4.1 and Cases 4.4-4.6 can represent various conditions of polymer-bitumen interaction. It can be seen that the four cases in Figure 4.6 all have different values of polymer volume fraction as the equilibrium phase composition. A lower χ value leads to a lower polymer fraction in the polymer-rich phase and higher polymer fraction in the bitumen-rich phase, whereas a higher z value results in a lower polymer fraction in the polymer-rich phase. This reflects the reality in PMBs. When the degree of polymer-bitumen interaction is higher, the PMB tends to form a more homogeneous blend. If the relative amount of interactive molecules in the bitumen is higher, more bitumen molecules can interact with the polymer chains and thus reduce the polymer fraction in the polymer-rich phase. Since the local composition dependency of χ has not been introduced into the model in this chapter, the effect of z on equilibrium phase composition is still not properly shown in the bitumen-rich phase in Figure 4.6.

In addition, Figure 4.6 also reveals that Case 4.5, with lower χ values than Case 4.6, takes longer time to reach the equilibrium state. This can be interpreted as an indication that with an increasing degree of polymer-bitumen interaction the separation process becomes more difficult. Last but not least, it is obvious from Figure 4.6 that the cases with higher z

values (Case 4.1 and Case 4.4) have higher area fractions of the polymer-rich phase in the results. This represents what actually happens in real PMBs. When the relative amount of interactive molecules in the bitumen is higher, more bitumen molecules can interact with the polymer chains and thus form more areas of polymer-rich phase in the PMB.

Besides the unstable cases (Cases 4.1-4.6), three stable cases (Cases 4.7-4.9) are also included in the parametric studies, as shown in Figure 4.7. Case 4.7 represents the thermodynamically unstable case with sufficiently low mobility and gradient energy coefficients. In this case, phase separation still happens in a very small scale. However, because of the extremely fine structure of the pseudo-binary blend, microscopy or other available experimental techniques may not be able to capture the structure and still recognize it as a stable case for the PMB. Cases 4.8 and 4.9 are the thermodynamically stable cases. Case 4.8 uses a $N\chi$ value less than 2.0, which means the degree of polymer-bitumen interaction is high enough to have a single well for the free energy of mixing. Thus, an absolutely homogeneous structure is formed in the PMB. Case 4.9 uses a very high z value and a relatively low $N\chi$ value (greater than but close to 2.0). This means the relative amount of interactive molecules in the bitumen is very high and the degree of polymer-bitumen interaction is relatively high but not high enough to have a single well for the free energy of mixing. So the simulated PMB can lie in the one-phase regime on the phase diagram and form an absolutely homogeneous structure.

5. Temperature Dependency of PMB Phase Separation Behaviour: Numerical Study

The phase separation behaviour of PMB is temperature-dependent, which means that a PMB may show different phase separation phenomena at different temperatures. This chapter aims to understand the temperature dependency of PMB phase separation behaviour and numerically investigates the effects of thermal condition on PMB phase separation.

5.1. Temperature Dependency of Model Parameters

Some previous studies (Soenen *et al.*, 2008, 2009; Lu *et al.*, 2010) have indicated that the thermal condition has important influences on the PMB microstructure. This means that the temperature level and its changing rate can significantly affect the phase separation behaviour of a PMB. However, a fundamental understanding on how these effects arise has still not yet been reached so far. In order to extend the model described above for a concerned temperature range instead of a single temperature point, the temperature dependency of the model parameters is introduced into the model in this chapter.

Some of the model parameters are dependent on temperature, controlling the temperature dependency of the PMB phase separation behaviour. This chapter considers the temperature dependency of the mobility coefficients (M), interaction and dilution parameters (χ and z). As the temperature dependency of the gradient energy coefficient (κ) may be quite weak (Cahn and Hilliard, 1958; Wen *et al.*, 2003), it is currently neglected in this chapter.

Theoretically, the mobility coefficients of different materials (polymer and bitumen) are related to their self-diffusion (or tracer diffusion) coefficients. According to the reported temperature dependency of the self-diffusion coefficient in a general form (Ertl and Dullien, 1973; Holz *et*

al., 2000), this chapter uses an Arrhenius temperature dependency for the mobility coefficients of polymer and bitumen, i.e.

$$M = M_0 e^{-\frac{E}{RT}}, \quad (5.1)$$

where M is the mobility coefficient; M_0 is the maximum mobility coefficient at infinite temperature; and E is the activation energy for mobility. Regarding the interaction parameter, it has been widely reported (Russell *et al.*, 1990; Chremos *et al.*, 2014) that the Flory-Huggins interaction parameter generally has the temperature dependency as

$$\chi = \frac{\alpha}{T} + \beta, \quad (5.2)$$

where α and β are respectively constants for the enthalpic and entropic contributions to the interaction parameter χ . As for the dilution parameter, it is related to the swelling ratio of the polymer modifier in PMB. Some researchers (Brûlé *et al.*, 1988) have reported that the polymer swelling ratio increases slightly in PMB, as the temperature increases. The dependency is approximately linear. This chapter thus uses a simple linear dependency for the dilution parameter, such that

$$z = kT + c, \quad (5.3)$$

where k and c are constants.

5.2. Model Calibration for Real PMBs

The finite element software COMSOL Multiphysics® has been used to implement the model described in the previous section. The geometry of the simulation domain is a rectangle of 2.5 mm × 2.0 mm meshed with triangular elements. This domain is basically the same size as the microscopic images (magnification 50×, by Soenen *et al.* (2009) and Lu *et al.* (2010)) that are used for calibration of the model parameters. The boundary condition and method for obtaining the initial values keep the same as in the previous chapter.

Four different PMBs (numbered 1-4) are simulated in this chapter with the intention of representing the four PMBs experimentally studied in Chapter 3 (same PMBs also investigated by Soenen *et al.* (2009) and Lu *et al.* (2010)). The needed parameters include the maximum mobility

coefficients (M_{p0} and M_{b0}), activation energies (E_p and E_b), gradient energy coefficient (κ), segment numbers of the chains (N_p and N_b) and the constants (α , β , k and c) for interaction and dilution parameters. In order to get the parameter values for the PMBs, the theoretical ranges of the model parameters discussed in Chapter 4 is considered before fixing the specific values. After this, the specific values are calibrated within the theoretical ranges of the model parameters by the comparison between the experimental and numerical results.

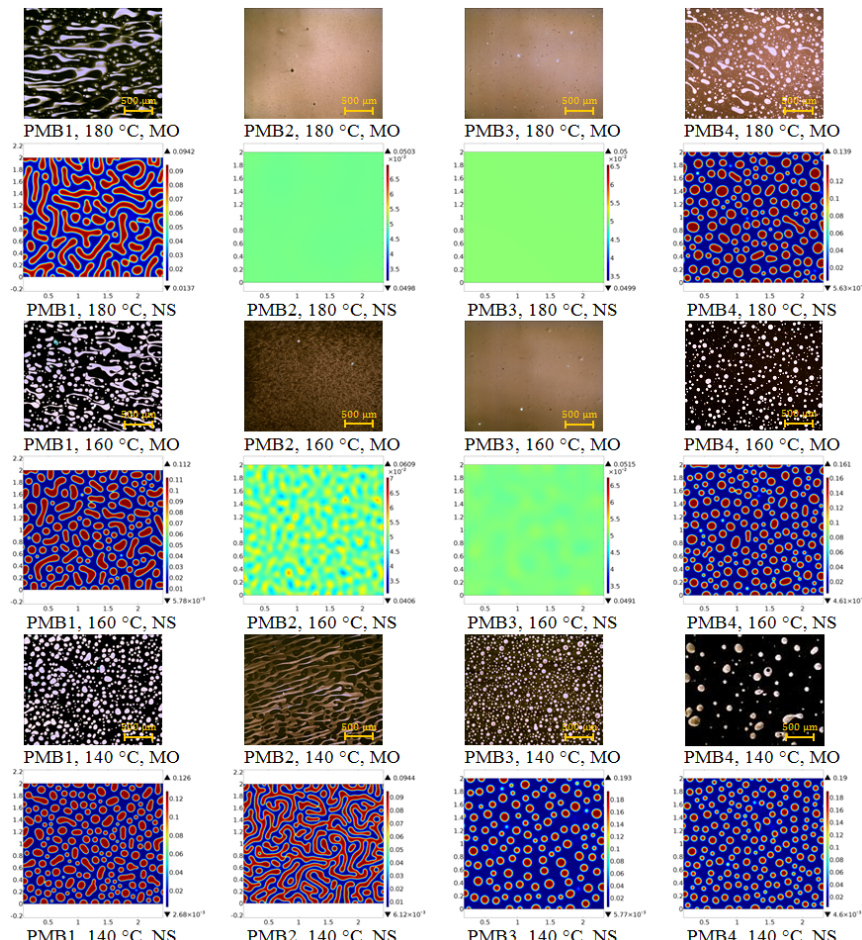


Figure 5.1. Microscopy observation (MO) and numerical simulation (NS) results of the four PMBs after 1 hour isothermal annealing.

Microscopy observation results by Soenen *et al.* (2009) and Lu *et al.* (2010) are used as the experimental corroboration for model calibration in this chapter. As presented in Figure 5.1, the microscopy images display the microstructure of the four PMBs after 1 hour isothermal annealing at 180 °C, 160 °C and 140 °C. It can be seen from the microscopy observation (MO) results in Figure 5.1 that the four PMBs show different phase separation behaviours. PMB1 and PMB4 separate into two phases at 180 °C (the lighter polymer-rich phase and the darker bitumen-rich phase), while PMB 2 and PMB3 remain homogeneous at this scale. At 140 °C, all the PMBs show two-phase structures but the patterns are different. For each of the PMBs, the microstructure changes as the temperature varies between 180 °C and 140 °C.

Table 5.1. The calibrated model parameters for the four PMBs.

Samples	M_{b0} [m ⁵ /(J·s)]	E_b [J/mol]	$N\alpha$ [K]	$N\beta$	k [K ⁻¹]	c
PMB1	2.1×10^{-14}	2.7×10^4	6.5×10^3	-11.8	3.75×10^{-2}	-7.7
PMB2	2.0×10^{-13}	3.7×10^4	7.6×10^3	-15.4	2.50×10^{-3}	8.9
PMB3	2.3×10^{-14}	2.3×10^4	1.6×10^4	-34.9	1.80×10^{-1}	-69.3
PMB4	1.2×10^{-16}	7.1×10^3	2.8×10^3	-2.7	4.50×10^{-2}	-13.4

In order to calibrate the model parameters for the four PMBs, the model described in the previous sections is implemented to reproduce these microscopy observation results. The numerical simulations represent the same condition as the experimental procedure by Soenen *et al.* (2009) and Lu *et al.* (2010). The calibrated model parameters are shown in Table 5.1, together with $M_{p0}=3.2 \times 10^{-14}$ m⁵/(J·s), $E_p=3.6 \times 10^4$ J/mol and $\kappa=4.50 \times 10^{-5}$ J/m. It is worth noting that in Table 5.1 the values of $N\alpha$ and $N\beta$ are obtained according to the estimated $N\chi$ values with the assumption of $N_p=N_b=N$ as described in Chapter 4. With these values, the numerical simulation (NS) results for the four PMBs are also shown in Figure 5.1, following the microscopy images. It is indicated that the phase separation behaviours of the PMBs are well reproduced by the model with the calibrated parameter values, including the stability differences between the PMBs and the microstructure differences between different temperatures. Thus, it is believed that the listed parameters in Table 5.1

can describe the phase separation behaviours of the four PMBs properly. However, the listed values are only valid for the studied temperature range, i.e. 140-180 °C. Beyond this range, more discussions are still needed.

The calibrated parameter values give the free energy curves by Equation 4.6. Consequently, a theoretical phase diagram of the four PMBs can be computed on the basis of the free energy curves. By plotting the free energy minimum points at different temperatures, the computed phase diagram of the four PMBs (the binodal curves) is obtained and presented in Figure 5.2. This phase diagram reveals the phase separation behaviours of the four PMBs within the studied temperature range. It will be discussed with the numerical simulation results in the following sections of this chapter.

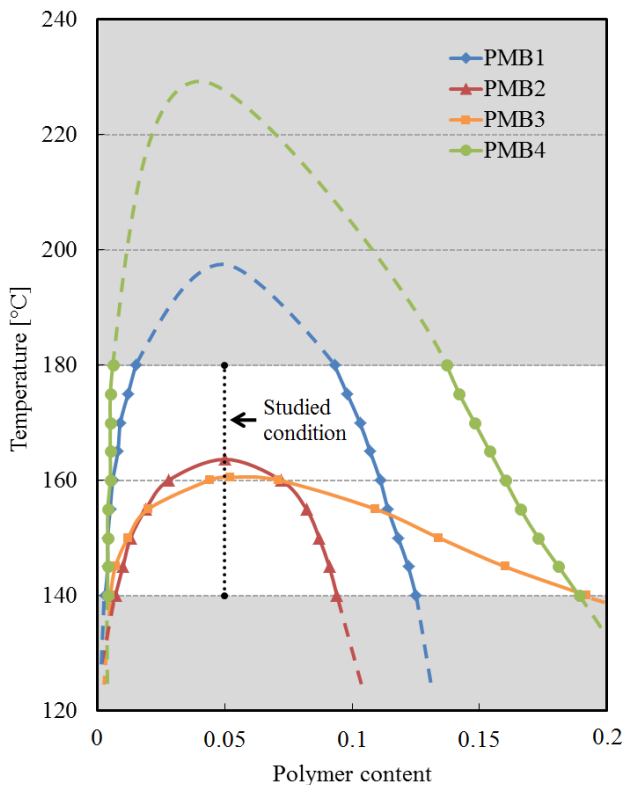


Figure 5.2. Computed phase diagram of the four PMBs.

5.3. Effect of Thermal Condition

The PMB phase separation is simulated under five different thermal conditions, numbered 1-5 as in Figure 5.3. They represent three different temperature levels ($180\text{ }^{\circ}\text{C}$, $160\text{ }^{\circ}\text{C}$ and $140\text{ }^{\circ}\text{C}$) and two cooling rates (fast cooling $8\text{ }^{\circ}\text{C}/\text{min}$ and slow cooling $2\text{ }^{\circ}\text{C}/\text{min}$) between $180\text{ }^{\circ}\text{C}$ and $140\text{ }^{\circ}\text{C}$. All the simulations are run to apply the thermal conditions for 4800 s.

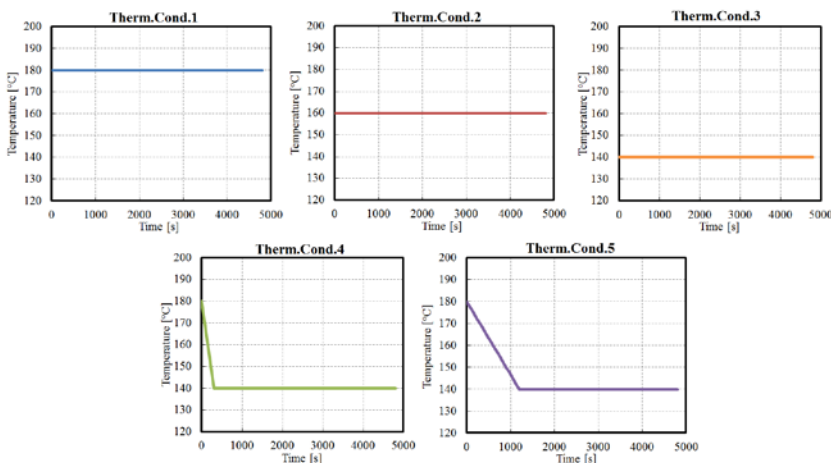


Figure 5.3. Thermal conditions applied in the simulations.

5.3.1. Effect of Temperature Level

The simulation results with Therm. Cond. 1-3 ($180\text{ }^{\circ}\text{C}$, $160\text{ }^{\circ}\text{C}$ and $140\text{ }^{\circ}\text{C}$) are shown in Figures 5.4-5.6 respectively. The results disclose the influence of temperature level on phase separation behaviour of the simulated PMBs. It can be seen in Figure 5.4 that PMB1 and PMB4 separate into two phases at $180\text{ }^{\circ}\text{C}$ (warmer colours for the polymer-rich phase and cooler colours for the bitumen-rich phase), while PMB2 and PMB3 have homogeneous structures even after the high temperature storage. According to Equation 5.2 and the material parameters, the $N\chi$ values of PMB1 and PMB4 are greater than 2.0 at $180\text{ }^{\circ}\text{C}$. Thus, their free energy curves are double wells at $180\text{ }^{\circ}\text{C}$, indicating their thermodynamic instability under Therm. Cond. 1. In contrast, PMB2 and PMB3 have $N\chi$ values less than 2.0, leading to their single-well free energy curves and thermodynamic stability under Therm. Cond. 1.

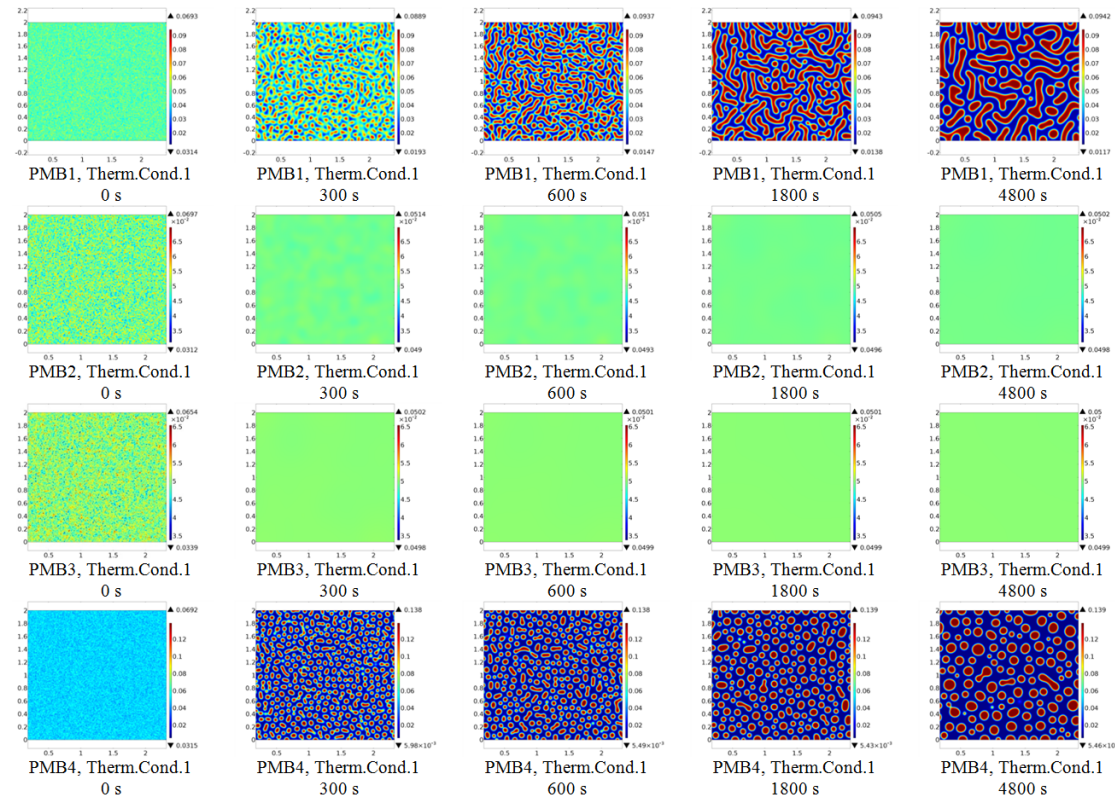


Figure 5.4. Numerical simulation results with ThermCond.1 (180 °C).

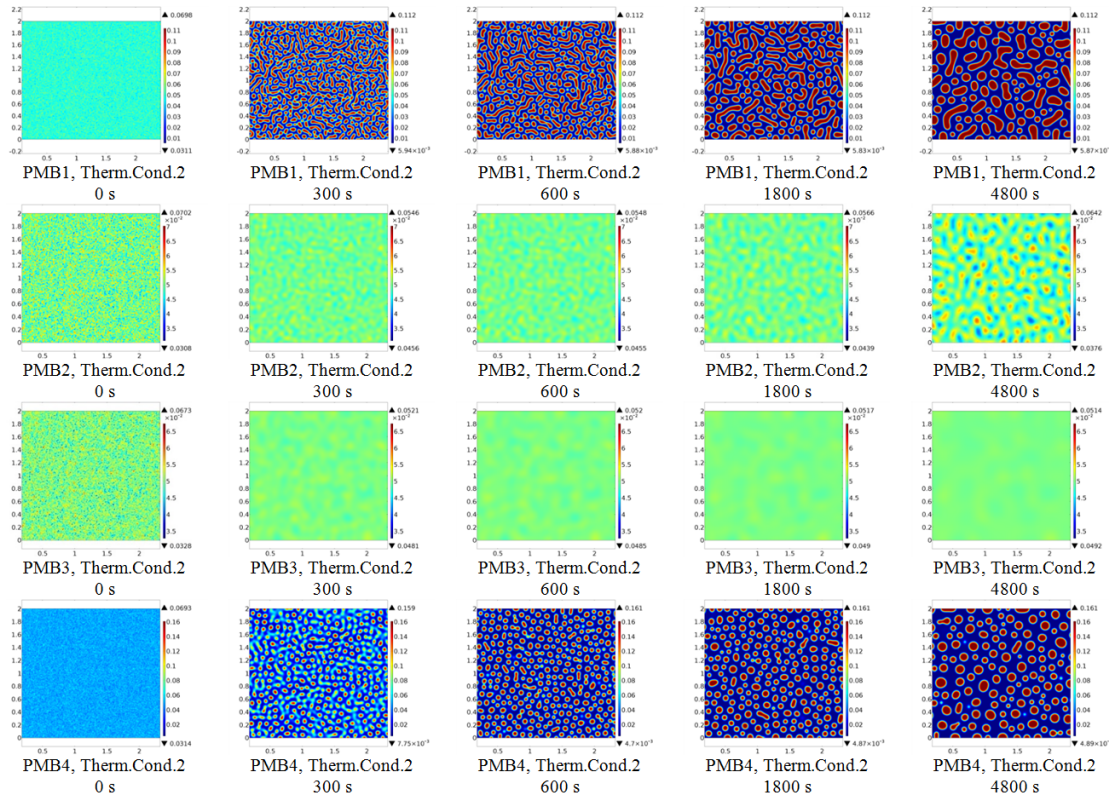


Figure 5.5. Numerical simulation results with ThermCond.2 (160 °C).

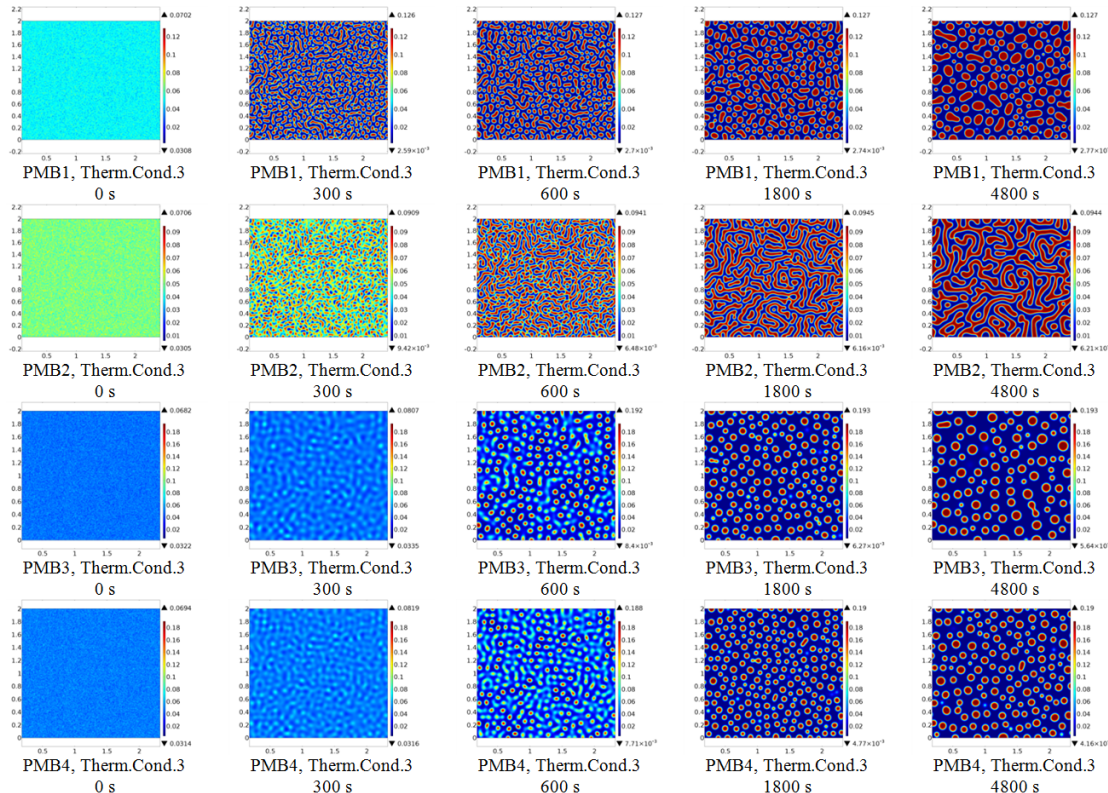


Figure 5.6. Numerical simulation results with ThermCond.3 (140 °C).

For the unstable PMB1 and PMB4, different patterns are shown in the simulation results with Therm.Cond.1. The polymer-rich phase forms threads in PMB1 but droplets in PMB4. This means the different base bitumen binders in PMB1 and PMB4 result in different swelling ratios of the polymer modifier, in spite of the same polymer content. According to Equation 5.3 and the material parameters, PMB1 has a higher dilution parameter than PMB4, showing a higher number of interactive molecules in the base bitumen of PMB1 than PMB4. This leads to the higher swelling ratio of the polymer in PMB1. In addition, Figure 5.4 gives the same values of equilibrium phase composition as indicated in Figure 5.2.

As the temperature decreases, PMB1 and PMB4 keep the two-phase structures but PMB2 and PMB3 become thermodynamically unstable through a stability-instability transition, shown in Figures 5.6 and 5.7. A lower temperature can only affect the microstructure and composition of the equilibrium phases in PMB1 and PMB4. But the temperature drop from 180 °C to 140 °C changes the stability of PMB2 and PMB3. At 140 °C, PMB2 and PMB3 have $N\chi$ values greater than 2.0 according to Equation 5.2 and the material parameters. This results in the double wells on their free energy curves and causes their phase separations under Therm.Cond.3. PMB2 and PMB3 show different patterns in Figure 5.6: a bicontinuous structure for PMB2 but a droplet pattern with a continuous matrix for PMB3. This can be attributed to the higher swelling ratio of the polymer in PMB2 than PMB3 at 140 °C, which is controlled by the dilution parameters. With Therm.Cond.2, Figure 5.5 displays the intermediate states of the PMBs during the thermodynamic transition between 180 °C and 140 °C.

In Figure 5.6, it is interesting to see that PMB3 and PMB4 show similar microstructures at 140 °C, although their phase structures are completely different with each other at other temperatures. This can be interpreted by the computed phase diagram Figure 5.2. At 180 °C, PMB3 lies in the one-phase regime of its phase diagram, but PMB4 is most possibly in its unstable regime. At 160 °C, the bimodal points of PMB3 are far away from those of PMB4. However, they come to almost the same locations at 140 °C. The different material parameters of PMB3 and PMB4 (as in Table 5.1) decide the different temperature dependencies of their phase separation behaviour. All these differences are expressed by the model and presented in the numerical simulation results. The same also applies for PMB1 and PMB2, and probably all PMBs.

5.3.2. Effect of Cooling Rate

The effect of temperature level on PMB phase separation behaviour is discussed in the previous section. However, PMB phase separation is essentially a time-dependent structure evolution process. Consequently, the changing rate of the temperature may also have its influence on PMB phase separation behaviour. Therm.Cond.4 and Therm.Cond.5 aim to investigate the effect of cooling rate on phase separation behaviour of the simulated PMBs. The simulation results are shown in Figures 5.7-5.11.

In Figure 5.7, it can be seen that PMB1 and PMB4 approximately follow a similar evolution routine as under the previous thermal conditions, although the fast cooling has its impacts on the separation process and the final PMB microstructure. But a homogenization process occurs in PMB2 and PMB3 during the fast cooling between 0 s and 300 s. This homogenization process is due to the transition of the PMBs from a thermodynamically stable state to a thermodynamically unstable state during the cooling. After the homogenization, PMB2 and PMB3 start to separate and form the binary structures at 140 °C.

Since the model presented in this chapter uses fixed material property parameters for a fixed temperature (e.g. 140 °C), it is not unexpected that the same temperature leads to the same equilibrium phase composition and polymer swelling ratio. As a consequence, the final patterns of the PMB binary structures in Figure 5.7 are quite similar as those in Figure 5.6, though not exactly the same. The final values of the local polymer volume fraction in the equilibrium phases in Figure 5.7 are the same as the final values in Figure 5.6, essentially controlled by the phase diagram of the four PMBs as Figure 5.2. However, the process can be more complicated in reality due to the potential effects of the interfacial tension, material viscosity and rheology.

Figures 5.8-5.11 show the PMB structure evolution processes under Therm.Cond.5 (with a lower cooling rate). According to Figures 5.8 and 5.11, both PMB1 and PMB4 start to separate from the very beginning of the simulated process. The results in Figures 5.8 and 5.11 indicate the influence of the bimodal point change (Figure 5.2) of the PMBs during the cooling. After the cooling termination at 1200 s, the PMBs reach the equilibrium states shown in Figure 5.2 but the final microstructures are slightly affected by the cooling rate.

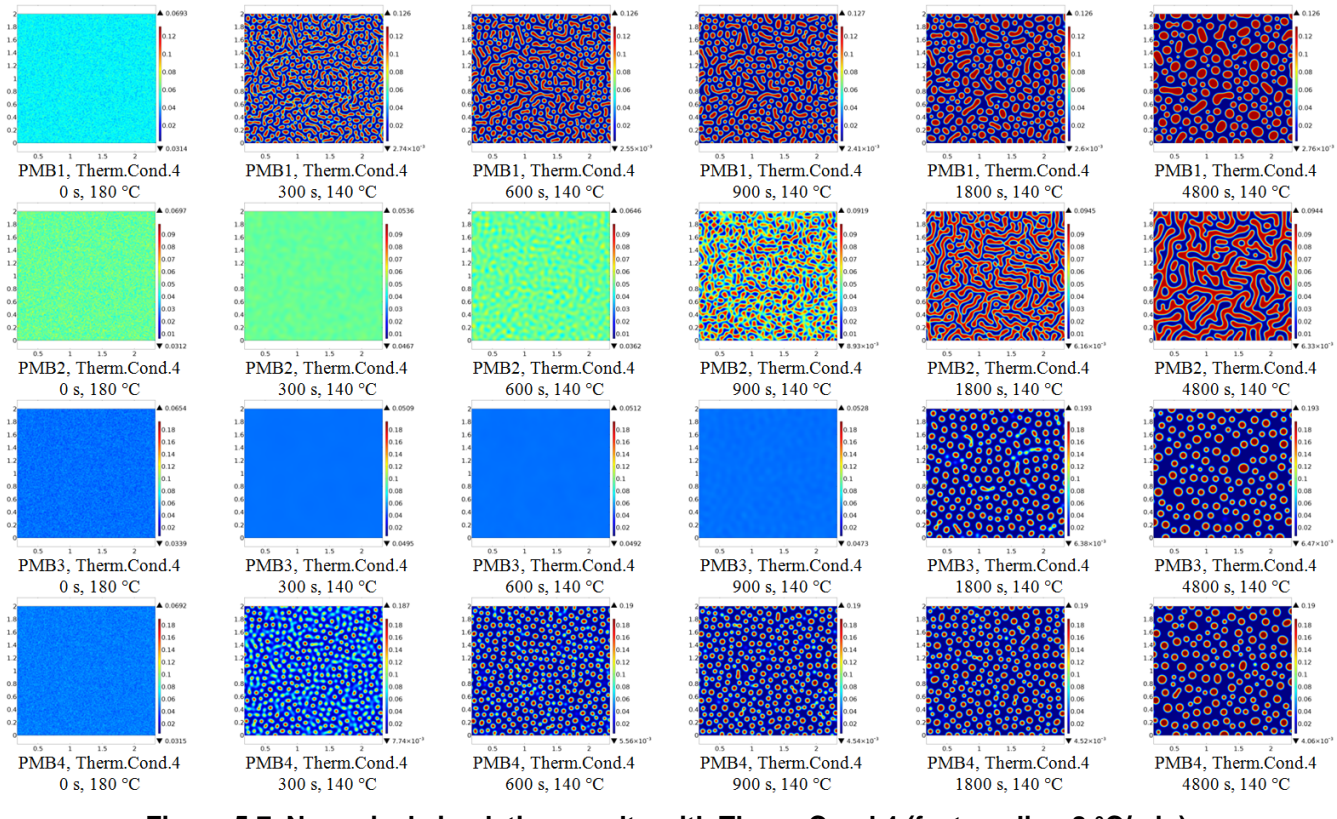


Figure 5.7. Numerical simulation results with Therm. Cond.4 (fast cooling 8 °C/min).

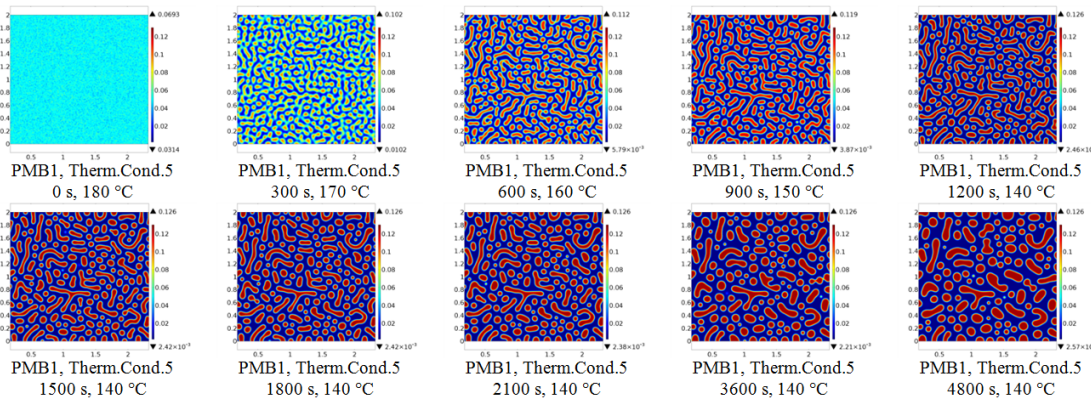


Figure 5.8. Numerical simulation results of PMB1 with Therm. Cond.5 (slow cooling 2 °C/min).

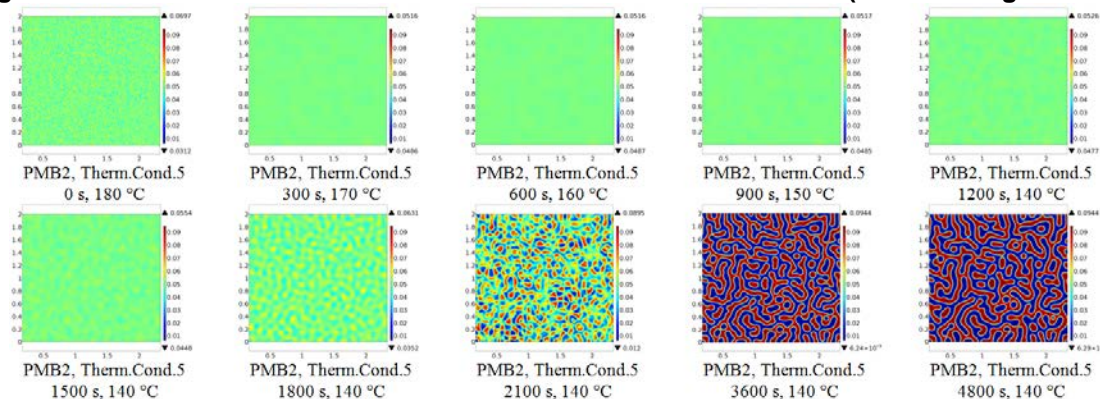


Figure 5.9. Numerical simulation results of PMB2 with Therm. Cond.5 (slow cooling 2 °C/min).

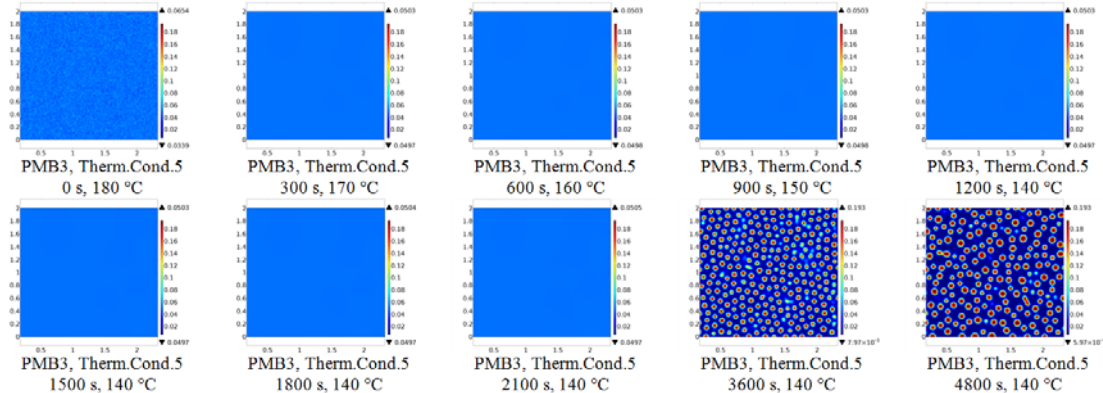


Figure 5.10. Numerical simulation results of PMB3 with ThermCond.5 (slow cooling 2 °C/min).

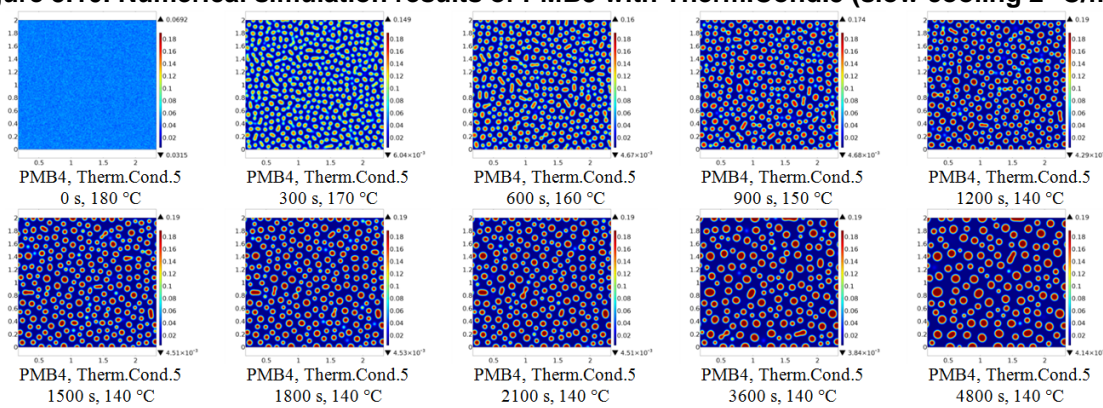


Figure 5.11. Numerical simulation results of PMB4 with ThermCond.5 (slow cooling 2 °C/min).

As for PMB2 and PMB3, Figure 5.2 reveals that their stability-instability transitions both occur between 170 °C (300 s) and 160 °C (600 s). Before the transitions, Figures 5.9 and 5.10 show that they form more homogenous structures than the initial ones. After the homogenization, the separation processes start and the PMBs gradually form the binary structures. As the phase separations start from more homogenized structures under Therm. Cond.5 than Therm. Cond.4, it takes longer time for the PMBs to reach the equilibrium states under Therm. Cond.5. By 2100 s (900 s after the cooling terminated), PMB3 has not displayed a two-phase structure in Figure 5.10. At the end of the simulated process, PMB2 and PMB3 reach the equilibrium states shown in Figure 5.2. However, the cooling rate only slightly affects the final patterns of the PMBs' binary structures in this chapter.

6. Diffusion-Flow Coupling and Its Effect on PMB Storage Stability

In the three-dimensional reality, PMB phase separation at the storage temperature is a coupled diffusion-flow process. The proposed phase-field model in the previous chapters demonstrates only the diffusion process related to the observed PMB phase separation by microscopy. On the basis of this diffusion model, this chapter presents a coupled diffusion-flow model and simulate the gravity-driven flow in PMB at the storage temperature.

6.1. Coupled Model of Diffusion and Flow

In order to simulate the gravity-driven flow in PMB at the storage temperature, the incompressible Navier-Stokes equations are coupled with the above formulated phase-field model. Since the discussed temperature is fixed in this chapter, the governing equations include only the mass and momentum conservation equations (not the energy conservation equation). Under the incompressible condition, the continuity equation in vector notation has the form of

$$\nabla \cdot \mathbf{u} = 0 , \quad (6.1)$$

where \mathbf{u} is the velocity vector. As this chapter is considering a two-dimensional model, the velocity is a two-component vector as $\mathbf{u} = (u, v)$. The equations of motion in vector notation can be written as

$$\rho \frac{\partial \mathbf{u}}{\partial t} + \rho(\mathbf{u} \cdot \nabla) \mathbf{u} = -\nabla p + \mu \nabla^2 \mathbf{u} + \mathbf{F} , \quad (6.2)$$

where ρ is the density; p is the pressure; μ is the dynamic viscosity; ∇^2 is the Laplace operator; and \mathbf{F} is the force vector. The force term \mathbf{F} can represent gravity, surface tension and/or other external forces. In this chapter, only gravity is considered for the force term.

It is worth mentioning that the incompressible Navier-Stokes equations presented here are based on some assumptions (Anderson, 1995; Hirsch, 2007). These assumptions also apply to the coupled diffusion-flow model for simulating the gravity-driven flow in PMB. Firstly, it is assumed that PMB is a Newtonian fluid at the storage temperature (180 °C). According to some previous studies (Sybilski, 1993, 1994; Garcia-Morales *et al.*, 2004, 2006; Navarro *et al.*, 2009), this assumption can be true when the polymer content is not too high and the temperature is sufficiently high. It was reported that a PMB with 5% (by weight) waste polymer showed Newtonian behaviour from 140 °C upwards in the range of the tested shear rates. Thus, it is believed that this first assumption is reasonable for common paving PMBs. In addition, it is also assumed by the equations that the gravity-driven flow in PMB at the storage temperature is a laminar flow. Because the PMB is at rest in the beginning of the modelled process and its viscosity is relatively high, this second assumption is also believed to be true for PMB in this case.

As a two-phase flow is introduced into the model, the governing equations become coupled with each other. With a velocity vector involved, Equation 4.1 can be rewritten into the complete form of the Cahn-Hilliard equation (Cahn and Hilliard, 1959; Yue *et al.*, 2004, 2006; Zhou *et al.*, 2010; Kim, 2012) as

$$\frac{\partial \phi}{\partial t} + \nabla \cdot \mathbf{u}\phi = \nabla \cdot M(\phi)\nabla \frac{\delta F}{\delta \phi}. \quad (6.3)$$

In Equation 6.2, the density ρ and dynamic viscosity μ are dependent on the local composition of the phase as well as the properties of the individual components. Under the incompressible condition, a linear dependency is postulated for the density in this chapter, such that

$$\rho(\phi) = \rho_p\phi + \rho_b(1 - \phi), \quad (6.4)$$

where ρ_p is the density of the polymer modifier; and ρ_b is the density of the bitumen. The empirical Kendall-Monroe equation (Kendall and Monroe, 1917; Viswanath *et al.*, 2007) is employed to estimate the dynamic viscosity of the phase, i.e.

$$\sqrt[3]{\mu(\phi)} = \sqrt[3]{\mu_p}\phi + \sqrt[3]{\mu_b}(1 - \phi), \quad (6.5)$$

where μ_p is the dynamic viscosity of the polymer modifier; and μ_b is the dynamic viscosity of the bitumen. As for the force term F , the following equation is used to represent the gravity, i.e.

$$\mathbf{F}(\emptyset) = \rho(\emptyset)\mathbf{g}, \quad (6.6)$$

where \mathbf{g} is the acceleration of gravity (vector).

6.2. Model Parameters and Implementation

The coupled diffusion-flow model described in the previous section has been implemented in the finite element software COMSOL Multiphysics®. The numerical simulations are performed on a rectangular domain of 1.2 mm × 2.7 mm meshed with triangular elements. This domain is in the vertical plane and basically three times the size of the microscopic images (magnification 100×) obtained in Chapter 3. The domain is equally divided into three parts (bottom, middle and top) for the data post-processing and analysis. Boundary conditions are set by having the velocity (both u and v) being zero on all the four sides of the rectangle and the pressure being zero on the top side. Initial values of \emptyset are generated by a normally distributed random function with a mean value of 0.05 and a standard deviation of 0.005. This means that the polymer content in the simulated PMB is 5% by volume with certain variation. If considering the density difference between the polymer and bitumen, the polymer content by weight is around 4.6%. The PMB is at rest ($u = v = 0$) in the beginning of the simulated process.

In order to simulate the gravity-driven flow in PMB at 180 °C, the needed parameters include the mobility coefficients (M_p and M_b), gradient energy coefficient κ , segment numbers of the chains (N_p and N_b), interaction parameter χ , dilution parameter z , densities (ρ_p and ρ_b) and dynamic viscosities (μ_p and μ_b). For N_p and N_b , it is assumed that the hypothetical chains for bitumen have the same length as the polymer chains, as discussed in the previous chapters. The values of M_p , M_b , κ , $N\chi$ and z can be calibrated by the comparison between the experimental and numerical results, while the values of ρ_p , ρ_b , μ_p and μ_b can be obtained by experimental measurements or using the related handbooks.

By setting different values for the material property parameters, the simulation cases listed in Table 6.1 are numerically implemented in this chapter for evaluating: (i) the capacity of the coupled diffusion-flow model to predict storage stability (and instability) of PMB, and (ii) the effects of bitumen density and dynamic viscosity on the gravity-driven

flow and phase separation in PMB at 180 °C. The values of ρ_p , ρ_b , μ_p and μ_b are assumed to be constant in Cases 6.1-6.3 and the used values are based on the material producer data documents, handbooks and reported data in the literature (Morgan and Mulder, 1995; Read and Whiteoak, 2003; Holden *et al.*, 1969; Arnold and Meier, 1970; Canevarolo *et al.*, 1986a, 1986b; Zeng and Wu, 2008; Wang *et al.*, 2012).

Moreover, the second part of the simulations (Cases 6.4-6.7) uses constant values (same as Case 6.1) for the diffusion model parameters (M_p , M_b , κ , $N\chi$ and z) and investigates the influences of the possible variations of the bitumen density ρ_b and dynamic viscosity μ_b . The used bitumen density and dynamic viscosity values, selected on the basis of the data from bitumen handbooks and the related literature (Morgan and Mulder, 1995; Read and Whiteoak, 2003; Zeng and Wu, 2008; Wang *et al.*, 2012), are intended to represent the most common bitumen grades. All the cases are run to simulate the storage at 180 °C for 5 hours.

Table 6.1. Material parameters used in the simulations (180 °C).

Cases	M_p [m ⁵ /(J·s)]	M_b [m ⁵ /(J·s)]	κ [J/m]	$N\chi$	z	ρ_p [kg/m ³]	ρ_b [kg/m ³]	μ_p [Pa·s]	μ_b [Pa·s]
6.1	6.00×10 ⁻¹⁸	6.75×10 ⁻¹⁸	4.50×10 ⁻⁵	2.9	8.7	855	932	2000	0.075
6.2	6.00×10 ⁻¹⁸	1.80×10 ⁻¹⁷	4.50×10 ⁻⁵	1.9	7.0	855	932	2000	0.075
6.3	6.00×10 ⁻¹⁸	1.80×10 ⁻¹⁷	4.50×10 ⁻⁵	3.6	7.0	855	932	2000	0.075
6.4	6.00×10 ⁻¹⁸	6.75×10 ⁻¹⁸	4.50×10 ⁻⁵	2.9	8.7	855	927	2000	0.075
6.5	6.00×10 ⁻¹⁸	6.75×10 ⁻¹⁸	4.50×10 ⁻⁵	2.9	8.7	855	937	2000	0.075
6.6	6.00×10 ⁻¹⁸	6.75×10 ⁻¹⁸	4.50×10 ⁻⁵	2.9	8.7	855	932	2000	0.05
6.7	6.00×10 ⁻¹⁸	6.75×10 ⁻¹⁸	4.50×10 ⁻⁵	2.9	8.7	855	932	2000	0.1

6.3. Numerical Simulation Results and Discussion

6.3.1. PMB Storage Stability

The simulation results of Cases 6.1-6.3 are shown in Figure 6.1. It can be seen that Case 6.2 represents a compatible case, and consequently, no separation happens in the simulated PMB. Thus, there is no two-phase structure formed and no density difference within the PMB. As a consequence, the gravity does not drive a flow in Case 6.2. With poor polymer-bitumen compatibility, Cases 6.1 and 6.3 start to separate into

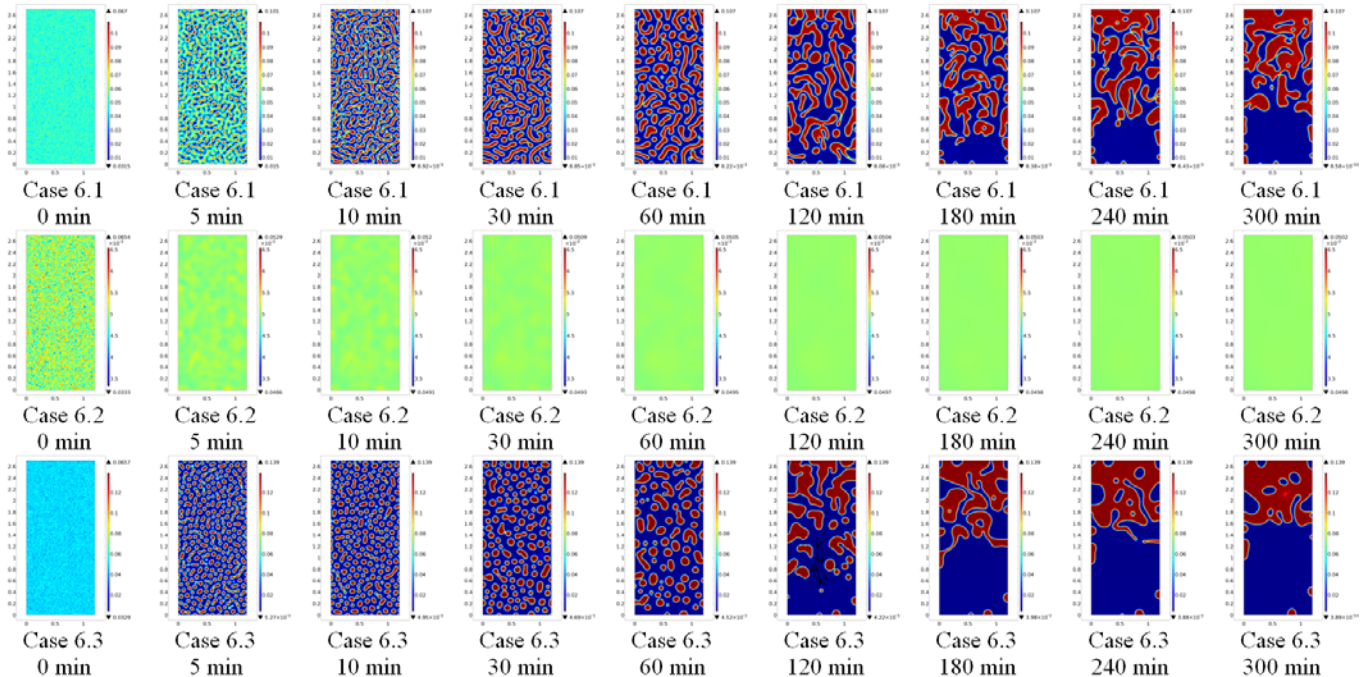


Figure 6.1. Simulation results of Cases 6.1-6.3.

two phases by diffusion. After the density difference between the two phases forms, the gravity starts to drive the flow of the two phases and accelerate the separation in the vertical direction.

Furthermore, the gravity-driven flow and phase separation can be analysed by measuring the polymer content changes in different parts of the domain during the whole simulated process. In this chapter, the domain is equally divided into three parts (bottom, middle and top). The average polymer contents (by volume) are calculated from the values of the phase-field variable in the three different parts and the results of Cases 6.1-6.3 are presented in Figure 6.2.

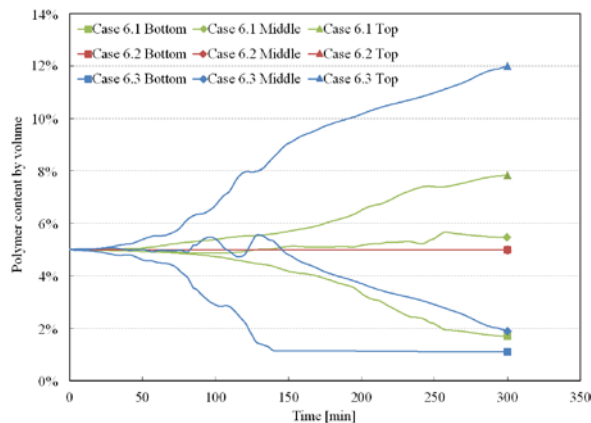


Figure 6.2. Polymer content (by volume) changes in the bottom, middle and top parts of the simulated PMBs, Cases 6.1-6.3.

Figure 6.2 gives the average contents of the pure polymer (not the polymer-rich phase) in different parts of the domain. It is indicated that the polymer contents in all the three parts of Case 6.2 always remain 5% by volume (i.e. the initial value, 4.6% by weight) during the simulation, showing the stability of this case. As for Cases 6.1 and 6.3, the polymer contents decrease in the bottom parts and increase in the top parts. This reveals the upward flows of the polymer-rich phases in both cases as the simulations continue. After 140 min, the polymer content reaches a plateau in the bottom part of Case 6.3. This is because almost all the polymer-rich phase has flowed to the upper parts from the bottom part, as seen in Figure 6.1. There are some polymer content fluctuations in the middle parts of Cases 6.1 and 6.3. The reason for these fluctuations is that

the middle parts of Cases 6.1 and 6.3 have both inflow and outflow of the polymer-rich phases. But since 140 min, there has been only the outflow (no inflow due to the plateau in the bottom) for the middle part of Case 6.3. Consequently, the polymer content in this part starts to decrease from 140 min.

It can also be seen in Figure 6.2 that Cases 6.1 and 6.3 show different gravity-driven flows and phase separation behaviours. The separation in Case 6.3 is faster than Case 6.1. This is because these two cases use different values for the diffusion model parameters, showing different bitumen mobility and leading to different composition of the equilibrium phases. The higher M_b value results in faster bitumen diffusion in Case 6.3. The bigger composition difference causes bigger density and dynamic viscosity differences between the two equilibrium phases of Case 6.3, which gives rise to a faster flow. Thus, Case 6.3 has separated more than Case 6.1 by the end of the simulated process.

6.3.2. Effect of Bitumen Density

Cases 6.4 and 6.5 are intended to investigate the effect of bitumen density variation. The simulation results show the same equilibrium phase composition and a similar separation process as the Case 6.1 results in Figure 6.1. However, the different bitumen density values lead to different levels of separation in Cases 6.4 and 6.5. The polymer content curves in

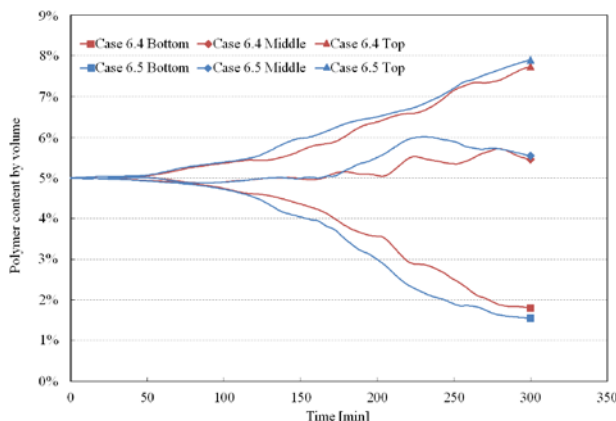


Figure 6.3. Polymer content (by volume) changes in the bottom, middle and top parts of the simulated PMBs, Cases 6.4 and 6.5.

different parts of the domain, as presented in Figure 6.3, give the explicit information on this. The bigger polymer-bitumen density difference causes a bigger density difference between the two equilibrium phases of Case 6.5, which results in a faster flow. Consequently, Case 6.5 has separated more than Case 6.4 by the end of the simulated process, although the difference between the two cases is limited.

6.3.3. Effect of Bitumen Dynamic Viscosity

Cases 6.6 and 6.7 are intended to investigate the effect of bitumen dynamic viscosity variation. The simulation results also show the same equilibrium phase composition and a similar separation process as the Case 6.1 results in Figure 6.1. However, the different bitumen dynamic viscosity values also lead to different levels of separation in Cases 6.6 and 6.7. The explicit information is given by the polymer content curves in different parts of the domain, as presented in Figure 6.4. The lower bitumen dynamic viscosity gives rise to lower dynamic viscosities of the two equilibrium phases of Case 6.6, which causes a faster flow. As a consequence, Case 6.6 has separated more than Case 6.7 by the end of the simulated process. The investigated variation of the dynamic viscosity μ_b seems to have a more significant influence than the investigated variation of the density ρ_b in this chapter. But this observation might depend on the specific values of the model parameters.

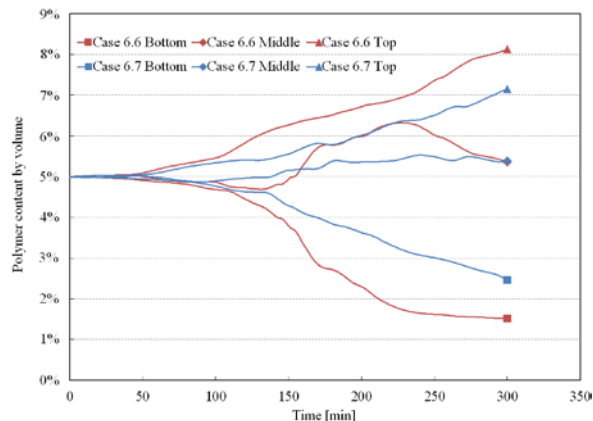


Figure 6.4. Polymer content (by volume) changes in the bottom, middle and top parts of the simulated PMBs, Cases 6.6 and 6.7.

7. Conclusions and Recommendations

7.1. Conclusions

Storage stability is a primary requirement for all PMBs, so understanding the stability-related phase behaviour of PMB is of great importance for supporting its successful application. The phase separation process in an unstable PMB is affected by many factors, e.g. the temperature, the bitumen composition, the polymer chemistry and content, the density and viscosity of the bitumen and polymer. Aiming at a fundamental understanding on what dictates the PMB storage stability and phase separation behaviour, this thesis reviews the advances and challenges in polymer modification of paving bitumen, experimentally captures the phase separation process in unstable PMBs and proposes a thermodynamic approach for PMB storage stability and phase separation prediction. A coupled phase-field model is developed to simulate the diffusion and flow processes related to PMB phase separation. The temperature dependency of PMB phase separation behaviour is discussed between 140 °C and 180 °C. On the basis of the above described results, the following conclusions can be drawn:

- (1) Storage stability and phase separation behaviour of PMB are strongly dependent on the specific combination of the base bitumen and polymer. A phase inversion phenomenon was experimentally observed in one of the investigated unstable PMBs during the phase separation. The plausible reason for this might be the dynamic asymmetry between the bitumen and polymer modifier. This indicates that viscoelastic phase separation may happen in some PMBs and the dynamic asymmetry should be evaluated when investigating PMB phase behaviour, especially at lower temperatures.
- (2) The proposed diffusion model, based on the Cahn-Hilliard equation and Flory-Huggins theory, is capable of capturing the

stability differences among the four investigated PMBs and their microstructure differences between different temperatures. The simulation results indicate that PMBs may show similar microstructures at one temperature, but their phase structures can be completely different at other temperatures. The different material parameters of the PMBs determine the differences in stability and temperature dependency of their phase separation behaviour. All these differences are captured by the model and demonstrated in the numerical simulation results. Depending on the stability-instability transition, a homogenization process may occur in some PMBs during cooling.

- (3) Experimental results indicate that the gravity effect due to polymer-bitumen density differences does not directly cause but accelerates the possible PMB phase separation process in the vertical direction. This means that an unstable PMB starts to separate into two phases by diffusion, because of the poor polymer-bitumen compatibility. Once the density difference between the two phases becomes sufficiently significant, gravity starts to drive the flow of the two phases and accelerate the separation in the vertical direction.
- (4) By employing the Navier-Stokes equations, the coupled model of diffusion and flow, can provide explicit information on the PMB phase separation due to the polymer-bitumen density differences. Simulation results reveal the upward flows of the polymer-rich phases in the unstable cases during the phase separation. There is no gravity-driven flow in the compatible case. The different gravity-driven phase separation behaviour of PMBs may result from the different composition of the equilibrium phases in the PMBs as well as the different densities and dynamic viscosities of the polymer and the bitumen. A bigger polymer-bitumen density difference and/or a lower bitumen dynamic viscosity cause a faster flow and separation in the PMB at storage temperature.

7.2. Recommendations

This thesis employs the phase-field method, a phenomenological method, to model and simulate the PMB phase behaviour at and near the storage

temperature. Some of the model parameters, as described in the respective chapters, are phenomenological parameters that need to be determined based on the results of experimental measurements and theoretical calculations. Due to the lack of available data for PMBs today, precise determination of material parameters still remains an issue. This issue may be resolved as more data will be released in the future together with further findings of potential empirical correlations between some easily-measurable parameters and the model parameters.

In addition, because of the complex chemical composition of bitumen, some assumptions and simplifications are made for the model development, which also cause some limitations of the current model. Examples have been mentioned in Chapter 4. In order to improve the model, future work could be focused towards introducing the dependency of some model parameters on the local composition. Furthermore, the expression of free energy for PMB may also be further studied, for example by analysing the relation between the solubility parameters of the individual materials and the free energy curve of the final PMB.

Regarding the temperature dependency of phase separation behaviour for a given PMB, it is the temperature that determines the final values of the polymer swelling ratio and equilibrium phase composition at the end of the simulated process in this thesis. This is because the presented model uses fixed material property parameters for a fixed temperature. However, the process can be more complex in reality due to the combined effects of the interfacial tension, material viscosity and rheology. The coupled diffusion-flow model may provide a solution for this by taking the interfacial tension and material viscosity into account, while the effect of material rheology has to be evaluated by investigating the dynamic asymmetry between the bitumen and polymer. However, before any such possible future work should be started, it is recommended that the developed coupled diffusion-flow model should firstly be validated via an experimental and numerical visualization of the gravity-driven flow in PMB at storage temperature, most probably at a larger scale to avoid scaling and boundary effects. Additionally, the composition dependency of PMB density, dynamic viscosity and mobility coefficient could also be further investigated for a wide range of PMBs to get a comprehensive overview of design parameters that may give practical guidance to bitumen engineers.

References

- Adedeji, A., Grünfelder, T., Bates, F. S., Macosko, C. W., Stroup-Gardiner, M., & Newcomb, D. E. (1996). Asphalt modified by SBS triblock copolymer: structures and properties. *Polymer Engineering & Science*, 36(12), 1707-1723.
- Airey, G. D. (2002). Rheological evaluation of ethylene vinyl acetate polymer modified bitumens. *Construction and Building Materials*, 16(8), 473-487.
- Airey, G. D. (2003). Rheological properties of styrene butadiene styrene polymer modified road bitumens. *Fuel*, 82(14), 1709-1719.
- Ameri, M., Mansourian, A., & Sheikhmotevali, A. H. (2012). Investigating effects of ethylene vinyl acetate and gilsonite modifiers upon performance of base bitumen using Superpave tests methodology. *Construction and Building Materials*, 36, 1001-1007.
- Arnold, K. R., & Meier, D. J. (1970). A rheological characterization of SBS block copolymers. *Journal of Applied Polymer Science*, 14(2), 427-440.
- Anders, D., & Weinberg, K. (2012). Thermophoresis in binary blends. *Mechanics of Materials*, 47, 33-50.
- Anders, D., Weinberg, K., & Reichardt, R. (2012). Isogeometric analysis of thermal diffusion in binary blends. *Computational Materials Science*, 52(1), 182-188.
- Anderson, J. D. (1995). *Computational Fluid Dynamics: The Basics with Applications*. New York: McGraw-Hill, Inc..
- Araki, T., & Tanaka, H. (2001). Three-dimensional numerical simulations of viscoelastic phase separation: Morphological characteristics. *Macromolecules*, 34(6), 1953-1963.
- Asphalt Institute, & Eurobitume. (2011). *The Bitumen Industry - A Global Perspective (2nd ed.)*. Lexington, Kentucky: Asphalt Institute; Brussels, Belgium: Eurobitume.

- Badalassi, V. E., Ceniceros, H. D., & Banerjee, S. (2003). Computation of multiphase systems with phase field models. *Journal of Computational Physics*, 190(2), 371-397.
- Becker, Y., Méndez, M. P., & Rodríguez, Y. (2001). Polymer modified asphalt. *Vision Tecnologica*, 9(1), 39-50.
- Brûlé, B. (1996). Polymer-modified asphalt cements used in the road construction industry: Basic principles. *Transportation Research Record: Journal of the Transportation Research Board*, 1535(1), 48-53.
- Brûlé, B., Brion, Y., & Tanguy, A. (1988). Paving asphalt polymer blends: Relationship between composition, structure and properties. In *Asphalt Paving Technology 1988: Journal of the Association of Asphalt Paving Technologists* (pp. 41-64). St. Paul, Minnesota: Association of Asphalt Paving Technologists.
- Cahn, J. W., & Hilliard, J. E. (1958). Free energy of a nonuniform system. I. Interfacial free energy. *The Journal of Chemical Physics*, 28(2), 258-267.
- Cahn, J. W., & Hilliard, J. E. (1959). Free energy of a nonuniform system. III. Nucleation in a two-component incompressible fluid. *The Journal of Chemical Physics*, 31(3), 688-699.
- Canevarolo, S. V., Birley, A. W., & Hemsley, D. A. (1986a). Effect of processing conditions on styrene-butadiene-styrene-thermoplastic rubber. *British Polymer Journal*, 18(1), 60-64.
- Canevarolo, S. V., Birley, A. W., & Hemsley, D. A. (1986b). Molten state transition in thermoplastic rubber. *British Polymer Journal*, 18(3), 191-195.
- Champion, L., Gerard, J.-F., Planche, J.-P., Martin, D., & Anderson, D. (2001). Low temperature fracture properties of polymer-modified asphalts relationships with the morphology. *Journal of Materials Science*, 36(2), 451-460.
- Chen, J. S., Liao, M. C., & Shiah, M. S. (2002). Asphalt modified by styrene-butadiene-styrene triblock copolymer: Morphology and model. *Journal of Materials in Civil Engineering*, 14(3), 224-229.
- Chen, L.-Q. (2002). Phase-field models for microstructure evolution. *Annual Review of Materials Research*, 32(1), 113-140.

- Chremos, A., Nikoubashman, A., & Panagiotopoulos, A. Z. (2014). Flory-Huggins parameter χ , from binary mixtures of Lennard-Jones particles to block copolymer melts. *The Journal of Chemical Physics*, 140(5), 054909.
- Collins, J. H., & Bouldin, M. G. (1992). Stability of straight and polymer-modified asphalts. *Transportation Research Record: Journal of the Transportation Research Board*, 1342(1), 92-100.
- Cong, Y., Huang, W., & Liao, K. (2008). Compatibility between SBS and Asphalt. *Petroleum Science and Technology*, 26(3), 346-352.
- Emerson, J. A., Toolan, D. T. W., Howse, J. R., Furst, E. M., & Epps III, T. H. (2013). Determination of solvent-polymer and polymer-polymer Flory-Huggins interaction parameters for poly (3-hexylthiophene) via solvent vapor swelling. *Macromolecules*, 46(16), 6533-6540.
- Ertl, H., & Dullien, F. A. L. (1973). Self-diffusion and viscosity of some liquids as a function of temperature. *AIChE Journal*, 19(6), 1215-1223.
- Flory, P. J. (1942). Thermodynamics of high polymer solutions. *The Journal of Chemical Physics*, 10(1), 51-61.
- Flory, P. J. (1953). *Principles of Polymer Chemistry*. Ithaca, NY: Cornell University Press.
- Fuentes-Audén, C., Sandoval, J. A., Jerez, A., Navarro, F. J., Martínez-Boza, F. J., Partal, P., & Gallegos, C. (2008). Evaluation of thermal and mechanical properties of recycled polyethylene modified bitumen. *Polymer Testing*, 27(8), 1005-1012.
- Galooyak, S. S., Dabir, B., Nazarbeygi, A. E., & Moeini, A. (2010). Rheological properties and storage stability of bitumen/SBS/montmorillonite composites. *Construction and Building Materials*, 24(3), 300-307.
- García-Morales, M., Partal, P., Navarro, F. J., Martínez-Boza, F., Gallegos, C., González, N., González, O., & Muñoz, M. E. (2004). Viscous properties and microstructure of recycled EVA modified bitumen. *Fuel*, 83(1), 31-38.
- García-Morales, M., Partal, P., Navarro, F. J., Martínez-Boza, F. J., & Gallegos, C. (2006). Process rheokinetics and microstructure of recycled EVA/LDPE-modified bitumen. *Rheologica Acta*, 45(4), 513-524.
- Giavarini, C., De Filippis, P., Santarelli, M. L., & Scarsella, M. (1996). Production of stable polypropylene-modified bitumens. *Fuel*, 75(6), 681-686.

- Hernández, G., Medina, E. M., Sánchez, R., & Mendoza, A. M. (2006). Thermomechanical and rheological asphalt modification using styrene-butadiene triblock copolymers with different microstructure. *Energy & Fuels*, 20(6), 2623-2626.
- Hirsch, C. (2007). *Numerical Computation of Internal and External Flows: The Fundamentals of Computational Fluid Dynamics (2nd Ed.)*. Oxford: Butterworth-Heinemann.
- Holden, G., Bishop, E. T., & Legge, N. R. (1969). Thermoplastic elastomers. *Journal of Polymer Science Part C: Polymer Symposia*, 26(1), 37-57.
- Holz, M., Heil, S. R., & Sacco, A. (2000). Temperature-dependent self-diffusion coefficients of water and six selected molecular liquids for calibration in accurate ^1H NMR PFG measurements. *Physical Chemistry Chemical Physics*, 2(20), 4740-4742.
- Hu, S. Y., & Chen, L.-Q. (2001). A phase-field model for evolving microstructures with strong elastic inhomogeneity. *Acta Materialia*, 49(11), 1879-1890.
- Huggins, M. L. (1942a). Theory of solutions of high polymers. *Journal of the American Chemical Society*, 64(7), 1712-1719.
- Huggins, M. L. (1942b). Some properties of solutions of long-chain compounds. *The Journal of Physical Chemistry*, 46(1), 151-158.
- Isacsson, U., & Lu, X. (1995). Testing and appraisal of polymer modified road bitumens - State of the art. *Materials and Structures*, 28(3), 139-159.
- Isacsson, U., & Lu, X. (1999). Characterization of bitumens modified with SEBS, EVA and EBA polymers. *Journal of Materials Science*, 34(15), 3737-3745.
- Kendall, J., & Monroe, K. P. (1917). The viscosity of liquids. II. The viscosity-composition curve for ideal liquid mixtures. *Journal of the American Chemical Society*, 39(9), 1787-1802.
- Kim, J. (2012). Phase-field models for multi-component fluid flows. *Communications in Computational Physics*, 12(3), 613-661.
- Kraus, G. (1982). Modification of asphalt by block polymers of butadiene and styrene. *Rubber Chemistry and Technology*, 55(5), 1389-1402.
- Kringos, N., Schmets, A., Scarpas, A., & Pauli, T. (2011). Towards an understanding of the self-healing capacity of asphaltic mixtures. *Heron*, 56(1/2), 45-74.
- Lewandowski, L. H. (1994). Polymer modification of paving asphalt binders. *Rubber Chemistry and Technology*, 67(3), 447-480.

- Li, Y., Li, L., Zhang, Y., Zhao, S., Xie, L., & Yao, S. (2010). Improving the aging resistance of styrene-butadiene-styrene tri-block copolymer and application in polymer-modified asphalt. *Journal of Applied Polymer Science*, 116(2), 754-761.
- Lindvig, T., Michelsen, M. L., & Kontogeorgis, G. M. (2002). A Flory-Huggins model based on the Hansen solubility parameters. *Fluid Phase Equilibria*, 203(1), 247-260.
- Lu, X., & Isacsson, U. (1997). Compatibility and storage stability of styrene-butadiene-styrene copolymer modified bitumens. *Materials and Structures*, 30(10), 618-626.
- Lu, X., Isacsson, U., & Ekblad, J. (1999). Phase separation of SBS polymer modified bitumens. *Journal of Materials in Civil Engineering*, 11(1), 51-57.
- Lu, X., Redelius, P., & Soenen, H. (2010). SBS modified bitumens: Does their morphology and storage stability influence asphalt mix performance? In *Proceedings of the 11th International Conference on Asphalt Pavements*, Nagoya, Japan, 1-6 August (pp. 1604-1613). Lino Lakes, MN: International Society for Asphalt Pavements.
- Lucena, M. C. C., Soares, S. A., & Soares, J. B. (2004). Characterization and thermal behavior of polymer-modified asphalt. *Materials Research*, 7(4), 529-534.
- Masson, J. F., Collins, P., Robertson, G., Woods, J. R., & Margeson, J. (2003). Thermodynamics, phase diagrams, and stability of bitumen-polymer blends. *Energy & Fuels*, 17(3), 714-724.
- Moelans, N., Blanpain, B., & Wollants, P. (2008). An introduction to phase-field modeling of microstructure evolution. *Calphad*, 32(2), 268-294.
- Morgan, P., & Mulder, A. (1995). *The Shell Bitumen Industrial Handbook*. Surrey: Shell Bitumen.
- Mouillet, V., Lamontagne, J., Durrieu, F., Planche, J. P., & Lapalu, L. (2008). Infrared microscopy investigation of oxidation and phase evolution in bitumen modified with polymers. *Fuel*, 87(7), 1270-1280.
- Navarro, F. J., Partal, P., García-Morales, M., Martín-Alfonso, M. J., Martínez-Boza, F., Gallegos, C., Bordado, J. C. M., & Diogo, A. C. (2009). Bitumen modification with reactive and non-reactive (virgin and recycled) polymers: A comparative analysis. *Journal of Industrial and Engineering Chemistry*, 15(4), 458-464.

- Oliver, J., Khoo, K. Y., & Waldron, K. (2012). The effect of SBS morphology on field performance and test results. *Road Materials and Pavement Design*, 13(1), 104-127.
- Ouyang, C., Wang, S., Zhang, Y., & Zhang, Y. (2005). Preparation and properties of styrene-butadiene-styrene copolymer/kaolinite clay compound and asphalt modified with the compound. *Polymer Degradation and Stability*, 87(2), 309-317.
- Painter, P. C. (1993). *The Characterization of Asphalt and Asphalt Recyclability* (Report ID: SHRP-A-675). Washington, DC: SHRP.
- Polacco, G., Berlincioni, S., Biondi, D., Stastna, J., & Zanzotto, L. (2005). Asphalt modification with different polyethylene-based polymers. *European Polymer Journal*, 41(12), 2831-2844.
- Polacco, G., Stastna, J., Biondi, D., & Zanzotto, L. (2006a). Relation between polymer architecture and nonlinear viscoelastic behavior of modified asphalts. *Current Opinion in Colloid & Interface Science*, 11(4), 230-245.
- Polacco, G., Muscente, A., Biondi, D., & Santini, S. (2006b). Effect of composition on the properties of SEBS modified asphalts. *European Polymer Journal*, 42(5), 1113-1121.
- Polacco, G., Filippi, S., Merusi, F., & Stastna, G. (2015). A review of the fundamentals of polymer-modified asphalts: Asphalt/polymer interactions and principles of compatibility. *Advances in Colloid and Interface Science*, 224, 72-112.
- Pérez-Lepe, A., Martínez-Boza, F. J., & Gallegos, C. (2007). High temperature stability of different polymer-modified bitumens: A rheological evaluation. *Journal of Applied Polymer Science*, 103(2), 1166-1174.
- Read, J., & Whiteoak, D. (2003). *The Shell Bitumen Handbook (5th Ed.)*. London: Thomas Telford Publishing.
- Redelius, P. G. (2000). Solubility parameters and bitumen. *Fuel*, 79(1), 27-35.
- Redelius, P. (2004). Bitumen solubility model using Hansen solubility parameter. *Energy & Fuels*, 18(4), 1087-1092.
- Redelius, P., & Soenen, H. (2015). Relation between bitumen chemistry and performance. *Fuel*, 140, 34-43.
- Russell, T. P., Hjelm Jr, R. P., & Seeger, P. A. (1990). Temperature dependence of the interaction parameter of polystyrene and poly(methyl methacrylate). *Macromolecules*, 23(3), 890-893.

- Sengoz, B., & Isikyakar, G. (2008a). Analysis of styrene-butadiene-styrene polymer modified bitumen using fluorescent microscopy and conventional test methods. *Journal of Hazardous Materials*, 150(2), 424-432.
- Sengoz, B., & Isikyakar, G. (2008b). Evaluation of the properties and microstructure of SBS and EVA polymer modified bitumen. *Construction and Building Materials*, 22(9), 1897-1905.
- Sengoz, B., Topal, A., & Isikyakar, G. (2009). Morphology and image analysis of polymer modified bitumens. *Construction and Building Materials*, 23(5), 1986-1992.
- Soenen, H., Lu, X., & Redelius, P. (2008). The morphology of bitumen-SBS blends by UV microscopy: An evaluation of preparation methods. *Road Materials and Pavement Design*, 9(1), 97-110.
- Soenen, H., Lu, X., & Redelius, P. (2009). The morphology of SBS modified bitumen in binders and in asphalt mix. In A. Loizos, M.N. Partl, T. Scarpas, & I.L. Al-Qadi (Eds.), *Advanced Testing and Characterization of Bituminous Materials: Proceedings of the 7th International RILEM Symposium ATCBM09*, Rhodes, Greece, 27-29 May (pp. 151-160). Leiden: CRC Press.
- Stastna, J., Zanzotto, L., & Vacin, O. J. (2003). Viscosity function in polymer-modified asphalts. *Journal of Colloid and Interface Science*, 259(1), 200-207.
- Sun, D., & Lu, W. (2006). Phase morphology of polymer modified road asphalt. *Petroleum Science and Technology*, 24(7), 839-849.
- Sybilska, D. (1993). Non-Newtonian viscosity of polymer-modified bitumens. *Materials and Structures*, 26(1), 15-23.
- Sybilska, D. (1994). Relationship between absolute viscosity of polymer-modified bitumens and rutting resistance of pavement. *Materials and Structures*, 27(2), 110-120.
- Tanaka, H., & Araki, T. (1997). Phase inversion during viscoelastic phase separation: Roles of bulk and shear relaxation moduli. *Physical Review Letters*, 78(26), 4966-4969.
- Ubachs, R. L. J. M., Schreurs, P. J. G., & Geers, M. G. D. (2004). A nonlocal diffuse interface model for microstructure evolution of tin-lead solder. *Journal of the Mechanics and Physics of Solids*, 52(8), 1763-1792.
- Vargas, M. A., Chávez, A. E., Herrera, R., & Manero, O. (2005). Asphalt modified by partially hydrogenated SBS tri-block copolymers. *Rubber Chemistry and Technology*, 78(4), 620-643.

- Varma, R., Takeichi, H., Hall, J. E., Ozawa, Y. F., & Kyu, T. (2002). Miscibility studies on blends of Kraton block copolymer and asphalt. *Polymer*, 43(17), 4667-4671.
- Viswanath, D. S., Ghosh, T. K., Prasad, D. H. L., Dutt, N. V. K., & Rani, K. Y. (2007). *Viscosity of Liquids: Theory, Estimation, Experiment, and Data*. Dordrecht: Springer.
- Wang, H., You, Z., Mills-Beale, J., & Hao, P. (2012). Laboratory evaluation on high temperature viscosity and low temperature stiffness of asphalt binder with high percent scrap tire rubber. *Construction and Building Materials*, 26(1), 583-590.
- Wang, T., Yi, T., & Yuzhen, Z. (2010). The compatibility of SBS-modified asphalt. *Petroleum Science and Technology*, 28(7), 764-772.
- Wen, G., Zhang, Y., Zhang, Y., Sun, K., & Fan, Y. (2002). Rheological characterization of storage-stable SBS-modified asphalts. *Polymer Testing*, 21(3), 295-302.
- Wen, Y. H., Simmons, J. P., Shen, C., Woodward, C., & Wang, Y. (2003). Phase-field modeling of bimodal particle size distributions during continuous cooling. *Acta Materialia*, 51(4), 1123-1132.
- Wloczysiak, P., Vidal, A., Papirer, E., & Gauvin, P. (1997). Relationships between rheological properties, morphological characteristics, and composition of bitumen-styrene butadiene styrene copolymers mixes. I. A three-phase system. *Journal of Applied Polymer Science*, 65(8), 1595-1607.
- Xia, T., Xu, J., Huang, T., He, J., Zhang, Y., Guo, J., & Li, Y. (2016). Viscoelastic phase behavior in SBS modified bitumen studied by morphology evolution and viscoelasticity change. *Construction and Building Materials*, 105, 589-594.
- Yildirim, Y. (2007). Polymer modified asphalt binders. *Construction and Building Materials*, 21(1), 66-72.
- Yue, P., Feng, J. J., Liu, C., & Shen, J. (2004). A diffuse-interface method for simulating two-phase flows of complex fluids. *Journal of Fluid Mechanics*, 515, 293-317.
- Yue, P., Zhou, C., Feng, J. J., Ollivier-Gooch, C. F., & Hu, H. H. (2006). Phase-field simulations of interfacial dynamics in viscoelastic fluids using finite elements with adaptive meshing. *Journal of Computational Physics*, 219(1), 47-67.
- Zanzotto, L., Stastna, J., & Vacin, O. (2000). Thermomechanical properties of several polymer modified asphalts. *Applied Rheology*, 10(4), 185-191.

- Zeng, M., & Wu, C. (2008). Effects of type and content of mineral filler on viscosity of asphalt mastic and mixing and compaction temperatures of asphalt mixture. *Transportation Research Record: Journal of the Transportation Research Board*, 2051(1), 31-40.
- Zhang, Y., Zhao, S., Li, Y., Xie, L., & Sheng, K. (2008). Radiation effects on styrene-butadiene-styrene copolymer. *Nuclear Instruments and Methods in Physics Research Section B: Beam Interactions with Materials and Atoms*, 266(15), 3431-3436.
- Zhou, C., Yue, P., Feng, J. J., Ollivier-Gooch, C. F., & Hu, H. H. (2010). 3D phase-field simulations of interfacial dynamics in Newtonian and viscoelastic fluids. *Journal of Computational Physics*, 229(2), 498-511.
- Zhou, D., Zhang, P., & Weinan, E. (2006). Modified models of polymer phase separation. *Physical Review E*, 73(6), 061801.
- Zhu, J., Chen, L.-Q., & Shen, J. (2001). Morphological evolution during phase separation and coarsening with strong inhomogeneous elasticity. *Modelling and Simulation in Materials Science and Engineering*, 9(6), 499-511.

Appended Papers